J. Fluid Mech. (1983), *vol.* 137, *pp.* 1–29
Printed in Great Britain

On the ability of drops or bubbles to stick to non-horizontal surfaces of solids

By E. B. DUSSAN V. AND ROBERT TAO-PING CHOW
Department of Chemical Engineering, University of Pennsylvania, Philadelphia, PA 19104

(Received 22 October 1982 and in revised form 25 March 1983)

It is common knowledge that relatively small drops or bubbles have a tendency to stick to the surfaces of solids. Two specific problems are investigated: the shape of the largest drop or bubble that can remain attached to an inclined solid surface; and the shape and speed at which it moves along the surface when these conditions are exceeded. The slope of the fluid–fluid interface relative to the surface of the solid is assumed to be small, making it possible to obtain results using analytic techniques. It is shown that from both a physical and mathematical point of view *contact-angle hysteresis*, i.e. the ability of the position of the contact line to remain fixed as long as the value of the contact angle θ lies within the interval $\theta_R \leqslant \theta \leqslant \theta_A$, where $\theta_A \not\equiv \theta_R$, emerges as the single most important characteristic of the system.

1. Introduction

The ability of drops or bubbles to stick to a non-horizontal solid surface is a phenomenon familiar to everyone. A foggy mirror in a steamy bathroom, gas bubbles lining the inside surface of a glass of water, or raindrops on windowpanes are just a few frequently observed examples. In addition, drops or bubbles are often found in various types of industrial equipment. It is in the latter case that questions of a quantitative nature frequently arise. For example, it is well known that condensation of vapour directly onto a relatively cool solid surface in the form of droplets can be as much as an order of magnitude more efficient than condensation onto a thin film of liquid covering the surface (Neumann, Abetelmessih & Hameed 1978). The rate of condensation is sensitive to both the size and shape of the drops, the smaller the drops, the faster the rate (Sadhal & Plesset 1979). It is thus important to identify the conditions under which drops can dislodge, roll off the surface and make way for the growth of smaller drops. Similarly, the presence of bubbles on a solid–liquid interface can have an undesirable effect. By reducing the area of contact between the liquid and the solid, their presence may slow down chemical reactions or reduce heat transfer rates. Yet another example consists of the spraying of chemicals such as pesticides. Here maximizing the area of coverage for a given volume of spray is desired (Furmidge 1962; Johnstone 1973).

The present work is concerned with (i) identifying the conditions under which a drop begins to roll down an inclined plane, and (ii) predicting its subsequent motion (see figure 1). The most crucial aspect of this problem from a modelling point of view is the identification of the 'glue' responsible for holding the drop onto the surface of the solid. It is appealing to think of the drop as being held in place by molecular forces arising from the solid. Also, that roughening the surface on a microscopic scale enhances the ability of the solid to 'grab' the drop. Although there is some truth in these statements, it is in general not profitable to use our intuition concerning the

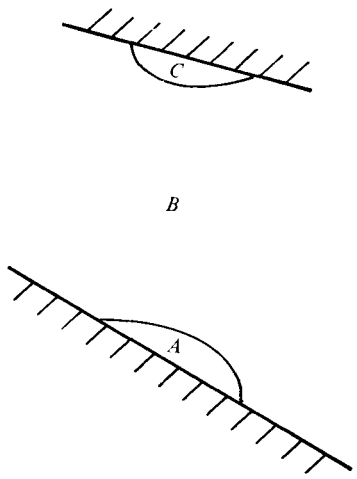

FIGURE 1. This study applies to the case when the density of fluid A is greater than the density of fluid B, or to the case when the density of fluid B is greater than the density of fluid C. Both cases are mathematically equal. The former corresponds to a drop, while the latter corresponds to a bubble.

adhesion of solids to other solids as a guide when dealing with drops on solid surfaces. All of the physical and chemical factors responsible for holding the drop onto the solid surface are lumped together in a continuum description by the specification of the *contact angle*. The contact angle under static and dynamic conditions determines the 'stickiness' of liquids to the solid surfaces. This study is based upon experimental observations of the behaviour of the contact angle.

Unfortunately, there presently exists some controversy concerning the validity of dynamic-contact-angle measurements. It has recently been shown (Ngan & Dussan V. 1982) that the contact angle measured in the usual way may not be its actual value. It has been speculated, based upon the results of various theoretical studies (Hansen & Toong 1971; Dussan V. 1976; Huh & Mason 1977; Kafka & Dussan V. 1979; Lowndes 1980) that the differences arise from the ability of the viscous forces to influence the shape of the fluid–fluid interface in the immediate vicinity of the moving contact line, even at values of the capillary number† as small as 10^{-2}. Hence, in order to minimize this effect, we restrict our analysis to contact-line speeds corresponding to *very small* capillary numbers. However, this does not eliminate the dependence of the contact angle on the speed of the contact line. Large variations may still occur due to the presence of non-equilibrium physical-chemical processes associated with the movement of molecules at the contact line (Blake & Haynes 1969).

In this study, we assume the contact angle θ depends on the speed U of the contact line as shown in figure 2. This incorporates (i) contact-angle hysteresis, and (ii) linear variations of the contact angle with the speed of the contact line. Thus, for stationary contact lines, $U = 0$, all values of θ within the internal $[\theta_R, \theta_A]$ are possible. Furthermore, when the liquid advances, $U > 0$ and $\theta = \theta_A + U/\kappa_A$, while if the liquid recedes, $U < 0$ and $\theta = \theta_R + U/\kappa_R$, with the value of κ_A not necessarily equal to that of κ_R. Four constants have been introduced, θ_A, θ_R, κ_A, κ_R, whose values depend on

† The capillary number is defined in §2. At this point, it is important to know that it is directly proportional to the speed of the contact line. For fluids with small viscosity, a small capillary number can correspond to a contact line moving at quite a substantial speed.

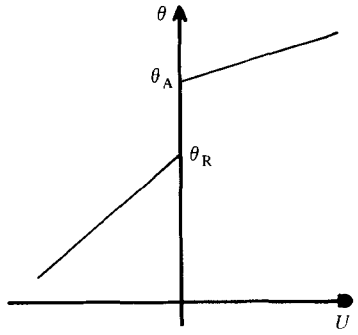

FIGURE 2. It is assumed that the advancing and receding contact angles depend only on the speed of the contact line. This model introduces four material constants: the advancing θ_A and receding θ_R contact angles (respectively the largest and smallest contact angles attainable under static conditions); and the values of the curve slopes $1/\kappa_A$ and $1/\kappa_R$, for $U > 0$ and $U < 0$ respectively.

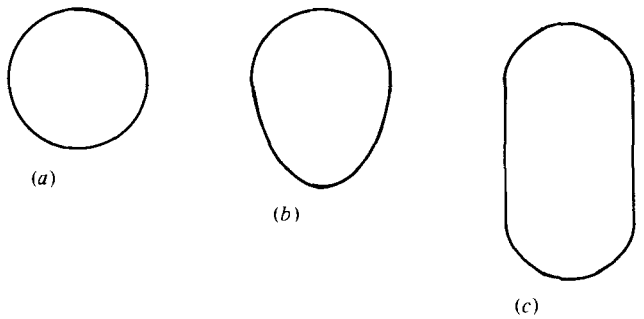

FIGURE 3. The shape of the contact line, as reported by Bikerman (1950) for a solid at three different angles of inclination. In (*a*) the solid is horizontal and the contact angle is θ_A. The solid is inclined slightly in (*b*), with its lowest end corresponding to the bottom of the figure. The contact line along the lower portion of the drop has advanced from its original position, while it has remained fixed along its upper portion. The angle of inclination is slightly greater than its critical value in (*c*).

the identity of the materials and the finish of the solid. In fact, the present work might be useful in defining experiments that allow one to measure all four of these material constants simultaneously.

Most of the literature concerned with drops on nonhorizontal surfaces consists of either analyses based upon *ad hoc* assumptions, or experimental measurements. MacDougall & Ockrent (1942) identify the importance of θ_A and θ_R in determining the critical angle of inclination of the solid, beyond which the drop moves continuously down its surface. By viewing drops from the side, they measure the contact angles at both the lowest and highest positions along the contact line. They find that these angles are always θ_A and θ_R, respectively, at the critical angle of inclination, independent of the initial shape of the drop. Bikerman (1950) reports on the evolving shape of the contact line for initially axisymmetric drops placed on a horizontal surface with constant contact angle θ_A (see figure 3). He reports that the slightest inclination of the solid caused the lowest portion of the drop to advance forward while the location of the contact line along the upper portion *remained fixed*. The drop achieves a static equilibrium configuration even though the contact line no longer has a circular shape. Only after the contact line achieves the shape depicted in figure 3(*c*), resulting from a further increase in the angle of inclination, does the drop

continue to move down the surface. This is also observed by Furmidge (1962). Furmidge also finds that a drop in its critical configuration satisfies the relation

$$\rho V g \sin\gamma_c = \omega\sigma(\cos\theta_R - \cos\theta_A), \tag{1.1}$$

where γ_c is the critical angle of inclination, V is the volume of the drop, ρ is the density of the liquid, ω is the width of the drop, g is the gravitational acceleration and σ is the surface tension. This relationship is exact, although Furmidge did not realize it despite the fact that it is in excellent agreement with his experiments. A derivation involving no *ad hoc* assumptions is given in Appendix A. Unfortunately, (1.1) is not predictive since the width ω of the drop is unknown. Hence further analysis is required.

Brown, Orr & Scriven (1980) analyse the shape of the drop when the contact line is *circular* with known radius. They identify the critical angle of inclination as that angle above which no solution exists to the equation describing the shape of the drop. This criterion is valid only for those *special cases* for which both the maximum and minimum values of the contact angle associated with the drop in its critical configuration (as they have defined it) are within the interval $[\theta_R, \theta_A]$. Clearly this is not the appropriate criterion for the drops in the experiments of both Bikerman and Furmidge. Although Brown *et al.* solved numerically the full nonlinear partial differential equation governing the shape of the interface, their problem is somewhat simplified by the fact that the location of the contact line is known *a priori*. Recently, Hocking (1981) has analysed the complete problem, as described by MacDougall & Ockrent, Bikerman and Furmidge, for two-dimensional thin drops. However, it is not obvious how one might apply his results to the three-dimensional case.

The boundary-value problem associated with the shape of the drop when the angle of inclination attains its critical value is not typical. There are two frequently encountered boundary conditions in the field of capillarity. The first involves the absence of contact-angle hysteresis, $\theta_A = \theta_R$, and the specification of the contact angle at the contact line. This is a free-boundary problem because the location of the contact line is not known *a priori*. The second involves a contact line of known location; here the contact angle is then determined as part of the solution. The only material systems which can achieve such a configuration are those for which $\theta_R \leqslant \theta \leqslant \theta_A$ for all values of θ on the contact line. The present problem of determining the critical configuration of the drop is shown in §2 to be a hybrid of the above two types. Over part of the boundary the contact angle is known while the location of the contact line is unknown, and over the remainder of the boundary the shape of the contact line is specified while the variation in value of the contact angle along its length is unknown. A peculiar feature of this problem is that part of the solution consists of determining the location of the points along the contact line at which this change in specification of the boundary condition occurs.

In §2 the general problem is formulated. Two special cases are identified and solved in §§3 and 4. In §5 a formal expansion is presented for the case of a drop moving slowly down an inclined surface, which is valid for materials characterized by $(\theta_A - \theta_R)/\theta_A \ll 1$. The expansion utilizes the solutions obtained in the previous two sections. A discussion of the results appears in §6.

2. Formulation

2.1. *Governing equations and boundary conditions*

Throughout this entire study, it is assumed that the slope of the fluid–fluid interface is everywhere small. This justifies using lubrication theory. Since we are only interested in the well-known lowest-order mode, the governing equations are presented without derivation and the dependent variables are not subscripted. The general formulation of this problem is quite similar to that of Greenspan (1978), who was interested in the spreading of a thin drop on a horizontal solid surface. However, the problems differ considerably due to the form of the boundary condition at the contact line and the necessity to include gravity in this study.

The equations governing the velocity and pressure fields, to lowest order, are

$$\left.\begin{aligned} \mathbf{0} &= -\nabla_{\mathrm{H}} P + \mu \frac{\partial^2 \boldsymbol{q}_{\mathrm{H}}}{\partial z^2} + \rho g \sin\gamma \boldsymbol{i}, \\ 0 &= -\frac{\partial P}{\partial z} - \rho g \cos\gamma, \end{aligned}\right\} \tag{2.1}$$

where P denotes the pressure, μ denotes the dynamic viscosity, $\nabla_{\mathrm{H}}(\,)$ denotes that portion of the gradient operator tangent to the surface of the solid, i.e. $\nabla_{\mathrm{H}}(\,) \equiv \boldsymbol{i}\,\partial(\,)/\partial x + \boldsymbol{j}\,\partial(\,)/\partial y$, and $\boldsymbol{q}_{\mathrm{H}}$ denotes that portion of the local velocity vector within the liquid drop tangent to the surface of the solid, i.e. $\boldsymbol{q}_{\mathrm{H}} = u(x,y,z)\,\boldsymbol{i} + v(x,y,z)\boldsymbol{j}$. The origin of the coordinate system lies on the surface of the solid, which is inclined at an angle γ with respect to the horizontal. Its x-axis lies tangent to and points down the surface, while the z-axis points in an upward direction perpendicular to the surface. The frame of reference is chosen to be at rest with respect to the centre of mass of the drop.

Other equations, boundary conditions and restrictions are as follows. The kinematic boundary condition and conservation of mass for an incompressible material combine to give

$$\frac{\partial h}{\partial t} + \nabla_{\mathrm{H}} \cdot (h\boldsymbol{Q}) = 0, \tag{2.2}$$

where $z = h(x,y,t)$ gives the location of the fluid–fluid interface, and $\boldsymbol{Q}$ is the height-averaged value of $\boldsymbol{q}_{\mathrm{H}}$:

$$\boldsymbol{Q} \equiv \frac{1}{h}\int_0^h \boldsymbol{q}_{\mathrm{H}}\,\mathrm{d}z. \tag{2.3}$$

The normal and tangential components of the dynamic boundary condition at the fluid–fluid interface are respectively

$$P = -\sigma \nabla_{\mathrm{H}}^2 h \quad \text{on} \quad z = h, \tag{2.4}$$

$$\frac{\partial \boldsymbol{q}_{\mathrm{H}}}{\partial z} = 0 \quad \text{on} \quad z = h. \tag{2.5}$$

It is assumed that the appropriate boundary condition at the drop–solid interface is the no-slip condition

$$\boldsymbol{q}_{\mathrm{H}} = \boldsymbol{U}_{\mathrm{P}} \quad \text{on} \quad z = 0. \tag{2.6}$$

where $\boldsymbol{U}_{\mathrm{P}}$ denotes the velocity of the plate relative to the centre of mass of the drop. Since we are only interested in the behaviour correct to $O(1)$ as the capillary number

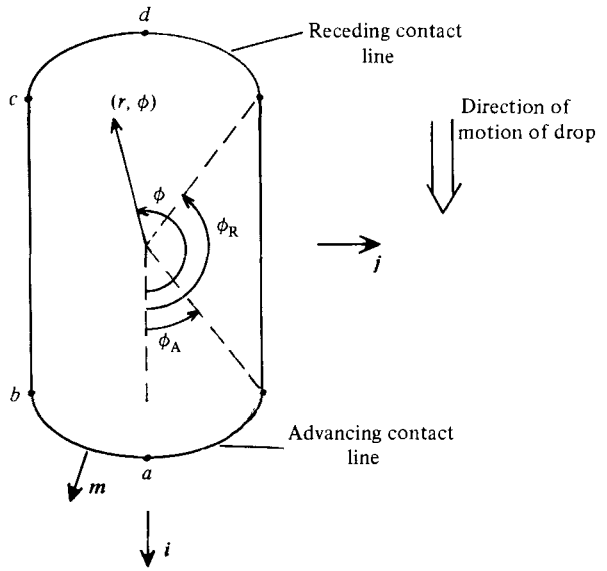

FIGURE 4. The plan view of the contact line when the angle of inclination is larger than its critical value causing the drop to move steadily down the surface. Both the polar coordinate system (r, ϕ) and the angular location of the ends of the straight-line segments of the contact line ϕ_A, ϕ_R, $2\pi-\phi_R$, $2\pi-\phi_A$ are identical.

approaches zero, the no-slip condition does not introduce a singularity at the moving contact line. And, finally, the volume V of the drop is fixed:

$$V = \int_S h \, ds, \tag{2.7}$$

where S denotes the drop–solid interface.

The heart of the problem lies in the proper handling of the boundary conditions at the contact line. Recall that we are primarily interested in the static configuration of the drop when the angle of inclination of the solid is at its critical value, and in the dynamics of the drop when the angle of inclination is somewhat larger than its critical value. The central point is realizing that for both cases segments of the contact line on both sides of the drop must be straight lines with unit tangents equal to $\boldsymbol{i}$, the direction of motion of the drop. This characteristic was present in the drawings of the shape of the contact line presented by both Bikerman and Furmidge, which were based upon their experimental observations; yet it was discussed by neither. The necessity of the existence of these straight-line segments becomes apparent when considering the problem from a theoretical point of view. Let's examine a drop moving down the surface at a constant speed U_D (expressed as $U_D \boldsymbol{i}$) as viewed from the frame of reference at rest with respect to the solid. The local speed of the contact line is by definition $\boldsymbol{U}_D \cdot \boldsymbol{m}$, where $\boldsymbol{m}$ is a unit vector lying in the tangent plane of the surface, perpendicular to the contact line, and pointing away from the drop (see figure 4). Its speed has a maximum positive value of U_0 at position a, gradually decreasing to zero at b. Along the entire straight-line segment, between b and c, the speed must be identically zero, gradually decreasing to a negative value of $-U_D$ at position d. The local value of the contact angle can be obtained from figure 2. Since the speed of the contact line is positive along the front of the drop, approaching zero at b, the value of the contact angle along that portion of the moving contact line must be greater

than θ_A, approaching the value of θ_A at b. Likewise, since the speed of the contact line is negative along its rear, the value of the contact angle must be less than θ_R approaching θ_R at c. If points b and c coincided, i.e. if the straight-line segment did not exist, then the contact angle would have to undergo a discontinuous change in value. Combining this with the requirement that the contact line possesses a continuous tangent gives rise to a singularity (see §4). Hence a segment of contact line is needed between positions c and b where the contact angle can continuously change in value from θ_R to θ_A. Recall, whenever the contact angle takes on values within this interval, the contact line must have zero speed (refer to figure 2). This is possible only if the tangent to the contact line points in the direction parallel to the motion of the drop. Thus, as the contact angle increases in value from θ_R to θ_A, the contact line must be a straight-line segment whose tangent points in the direction of motion of the drop. It might be possible for a moving contact line to exist with a discontinuity in its local tangent sector. However, this is outside the scope of the present study. In §4 it is shown that such shapes would be inconsistent with the small-slope approximation.

It follows from the above discussion that along the contact line

$$(\hat{\boldsymbol{U}}-\boldsymbol{U}_P)\cdot\boldsymbol{m} = \begin{cases} \kappa_A(\theta-\theta_A) & \text{for} \quad -\phi_A < \phi < \phi_A, \\ 0 & \text{for} \quad \phi_A < \phi < \phi_R, \\ \kappa_R(\theta-\theta_R) & \text{for} \quad \phi_R < \phi < 2\pi-\phi_R, \\ 0 & \text{for} \quad 2\pi-\phi_R < \phi < 2\pi-\phi_A, \end{cases}$$

$$\text{contact line is a straight-line segment} \quad \begin{cases} \phi_A < \phi < \phi_R, \\ 2\pi-\phi_R < \phi < 2\pi-\phi_A, \end{cases}$$

where $\hat{\boldsymbol{U}}$ denotes the velocity of the contact line measured in the frame of reference which is at rest with the centre of mass of the drop, and (r,ϕ) denotes a polar coordinate system in the $z=0$ plane (refer to figure 4). The values of ϕ, i.e. ϕ_A and ϕ_R, at which the nature of the boundary condition changes, are not known *a priori*.

Integrating (2.1) and applying the boundary conditions expressed in (2.4)–(2.6) enables us to evaluate (2.3), yielding

$$\boldsymbol{Q} = \frac{h^2}{3\mu}\{\sigma\boldsymbol{\nabla}_H\nabla_H^2 h - \rho g\cos\gamma\boldsymbol{\nabla}_H h + \rho g\sin\gamma\boldsymbol{i}\} + \boldsymbol{U}_P. \tag{2.8}$$

Substituting the above expression into (2.2) gives

$$\frac{\partial h}{\partial t} + \boldsymbol{\nabla}_H\cdot\left\{\frac{h^3}{3\mu}[\sigma\boldsymbol{\nabla}_H\nabla_H^2 h - \rho g\cos\gamma\boldsymbol{\nabla}_H h + \rho g\sin\gamma\boldsymbol{i}] + \boldsymbol{U}_P h\right\} = 0. \tag{2.9}$$

The boundary condition at the contact line can be rewritten as

$$(\hat{\boldsymbol{U}}-\boldsymbol{U}_P)\cdot\boldsymbol{\nabla}_H h = \begin{cases} -\kappa_A|\boldsymbol{\nabla}_H h|^2\left(\dfrac{1-\theta_A}{|\boldsymbol{\nabla}_H h|}\right) & \text{for} \quad -\phi_A < \phi < \phi_A, \\ 0 & \text{for} \quad \phi_A < \phi < \phi_R, \\ -\kappa_R|\boldsymbol{\nabla}_H h|^2\left(\dfrac{1-\theta_R}{|\boldsymbol{\nabla}_H h|}\right) & \text{for} \quad \phi_R < \phi < 2\pi-\phi_R, \\ 0 & \text{for} \quad 2\pi-\phi_R < \phi < 2\pi-\phi_A, \end{cases} \tag{2.10}$$

$$\text{contact line is a straight-line segment} \quad \begin{cases} \phi_A < \phi < \phi_R, \\ 2\pi-\phi_R < \phi < 2\pi-\phi_A, \end{cases}$$

where we have used $\boldsymbol{m} = -\nabla_{\mathrm{H}} h/|\nabla_{\mathrm{H}} h|$ and $\theta \approx \tan\theta = |\nabla_{\mathrm{H}} h|$ evaluated at the contact line, $h = 0$, the latter being consistent with the small-slope approximation. Typical of free-surface problems solved using the lubrication approximation, the shape h of the interface emerges as the sole unknown dependent variable. The location of the contact line, ϕ_{A}, ϕ_{R} and $\boldsymbol{U}_{\mathrm{P}}$ are also unknown.

2.2. *Scaling and identification of boundary-value problems*

The lengthscale for both the x- and y-variables is denoted by a. This represents the radius of the circular area of the solid wetted by a drop placed symmetrically with constant contact angle θ_{A} on a surface inclined at an angle γ neglecting the influence of gravity in the direction $\boldsymbol{i}$ tangent to the surface. The variables z and h are scaled with $\theta_{\mathrm{A}} a$. Since any motion is a direct consequence of the behaviour of the dynamic contact angle, all the velocities are scaled by $\kappa_{\mathrm{A}}\theta_{\mathrm{A}}$. Time is scaled by $a/\kappa_{\mathrm{A}}\theta_{\mathrm{A}}$. Defining dimensionless variables based upon these scales and substituting them into (2.7)–(2.10) yields

$$\int_S h \,\mathrm{d}S = \frac{V}{a^3\theta_{\mathrm{A}}}, \tag{2.11}$$

$$\boldsymbol{Q} = \frac{h^2}{C_{\mathrm{a}}}\{\nabla_{\mathrm{H}}\nabla_{\mathrm{H}}^2 h - T\nabla_{\mathrm{H}} h + G\boldsymbol{i}\} + \boldsymbol{U}_{\mathrm{P}}, \tag{2.12}$$

$$\frac{\partial h}{\partial t} + \nabla_{\mathrm{H}}\cdot\left\{\frac{h^3}{C_{\mathrm{a}}}[\nabla_{\mathrm{H}}\nabla_{\mathrm{H}}^2 h - T\nabla_{\mathrm{H}} h + G\boldsymbol{i}] + \boldsymbol{U}_{\mathrm{P}}\right\} = 0, \tag{2.13}$$

$$(\hat{\boldsymbol{U}} - \boldsymbol{U}_{\mathrm{P}})\cdot\nabla_{\mathrm{H}} h = \begin{cases} -|\nabla_{\mathrm{H}} h|^2\left(1 - \dfrac{1}{|\nabla_{\mathrm{H}} h|}\right) & \text{for} \quad -\phi_{\mathrm{A}} < \phi < \phi_{\mathrm{A}}, \\ 0 & \text{for} \quad \phi_{\mathrm{A}} < \phi < \phi_{\mathrm{R}}, \\ -\dfrac{\kappa_{\mathrm{R}}}{\kappa_{\mathrm{A}}}|\nabla_{\mathrm{H}} h|^2\left(1 - \dfrac{1-\epsilon}{|\nabla_{\mathrm{H}} h|}\right) & \text{for} \quad \phi_{\mathrm{R}} < \phi < 2\pi - \phi_{\mathrm{R}}, \\ 0 & \text{for} \quad 2\pi - \phi_{\mathrm{R}} < \phi < 2\pi - \phi_{\mathrm{A}}, \end{cases} \tag{2.14}$$

where all the above variables are now dimensionless; the capillary number C_{a} is $3\mu\kappa_{\mathrm{A}}/\sigma\theta_{\mathrm{A}}^2$, the hysteresis parameter ϵ is $(\theta_{\mathrm{A}} - \theta_{\mathrm{R}})/\theta_{\mathrm{A}}$, and the two gravitational parameters T and G are defined as $\rho g a^2 \cos\gamma/\sigma$ and $\rho g a^2 \sin\gamma/\sigma\theta_{\mathrm{A}}$ respectively.

As stated earlier, we are restricting this study to the limiting case valid to $O(1)$ as $C_{\mathrm{a}} \to 0$. Assuming that the proper expansion for h is

$$h(r, \phi; C_{\mathrm{a}}, g, \epsilon, T, \kappa_{\mathrm{A}}/\kappa_{\mathrm{R}}) = h_0(r, \phi; G, \epsilon, T, \kappa_{\mathrm{A}}/\kappa_{\mathrm{R}}) + o(1)$$

as $C_{\mathrm{a}} \to 0$ and that $\boldsymbol{Q} = O(1)$ as $C_{\mathrm{a}} \to 0$, (2.12) gives

$$\nabla_{\mathrm{H}}^2 h_0 - T h_0 + G x = A_0, \tag{2.15}$$

where the constant of integration $A_0(G, \epsilon, T, \kappa_{\mathrm{A}}/\kappa_{\mathrm{R}})$ must be determined. Note that (2.15) can also be obtained by substituting the above expansion for h into (2.13). It is not surprising that (2.15) is the same as the equation that would be derived under static conditions. Hence the dynamics of the problem enters entirely through the boundary condition given by (2.14). The above derivation of (2.15) follows Greenspan, who was also concerned with the behaviour of a thin drop correct to $O(1)$ as $C_{\mathrm{a}} \to 0$.

Although the governing partial differential equation (2.15) is linear, the entire problem is nonlinear owing to the form of the boundary condition (2.14). In order to make the problem tractable from an analytic point of view, the investigation is restricted to material systems for which ϵ is small, and to angles of inclination above its critical value, for which $G - G_{\mathrm{c}}$ is small, where $G_{\mathrm{c}} \equiv \rho g a^2 \sin\gamma_{\mathrm{c}}/\sigma\theta_{\mathrm{A}}$.

Solutions to two limiting cases are obtained. In §3, we look at the limit when $G \to 0$ and $\epsilon \equiv 0$. Here the dependence of the speed and shape of the drop on κ_A and κ_R is determined. In §4 the shape of the drop is analysed when the angle of inclination is at its critical value, i.e. $G = G_c$ and $\epsilon \to 0$. Finally, in §5, the two limiting cases are combined to give a solution to the general problem of a drop moving down an inclined plane at a constant speed, in which $\epsilon \not\equiv 0$.

In the remainder of this section the solution for the case when $\epsilon \equiv 0$ and $G \equiv 0$, denoted as the (000)-mode, is presented since it is needed in both §§3 and 4. Note that solutions corresponding to small values of G can represent either small drops on surface inclined at any angle $0° \leqslant \gamma \leqslant 90°$ or large drops on almost horizontal surfaces. Hence the (000) mode is *not* limited to describing the shapes of drops on only horizontal surfaces.

2.3. *Solution to* (000)*-mode*

At the limit $\epsilon \equiv 0$ and $G \equiv 0$, (2.15) becomes

$$\nabla_H^2 h_{000} - T h_{000} = A_{000}.$$

Since the static contact angle is unique, the contact line must be circular with constant radius, and the shape of the drop must be symmetric about its vertical axis. Hence in dimensionless form this gives

$$h_{000}(1) = 0, \tag{2.16}$$

$$\frac{d^2 h_{000}}{dr^2} + \frac{1}{r}\frac{dh_{000}}{dr} - T h_{000} = A_{000}. \tag{2.17}$$

The contact-angle boundary condition (2.14) is

$$\frac{dh_{000}}{dr} = -1 \quad \text{on} \quad r = 1. \tag{2.18}$$

It is easily established that the solution to (2.16)–(2.18) is

$$h_{000} = \frac{I_0(T^{\frac{1}{2}}) - I_0(rT^{\frac{1}{2}})}{T^{\frac{1}{2}} I_1(T^{\frac{1}{2}})}, \tag{2.19}$$

$$A_{000} = -\frac{T^{\frac{1}{2}} I_0(T^{\frac{1}{2}})}{I_1(T^{\frac{1}{2}})}, \tag{2.20}$$

where I_0 and I_1 are the modified Bessel functions (Abramowitz & Stegun 1964), and where we have made use of the usual requirement of boundedness at $r = 0$. Substituting (2.19) into (2.11) gives

$$\frac{V}{a^3 \theta_A} = \frac{\pi I_0(T^{\frac{1}{2}})}{T^{\frac{1}{2}} I_1(T^{\frac{1}{2}})} - \frac{2\pi}{T}. \tag{2.21}$$

3. The steady motion of a drop moving down an inclined plane with no contact-angle hysteresis

3.1. *Formulation of boundary-value problem*

When there is no contact-angle hysteresis, i.e. $\epsilon = 0$, any inclination of the solid, no matter how small, will cause a drop to move down its surface. In addition, there is no reason to anticipate the appearance of the straight-line segments on the sides of the drop because the dependence of the contact angle on U is continuous at $U = 0$.

A regular expansion in G is assumed for the dependent variable h_0 and the parameters A_0 and $\boldsymbol{U}_{\mathrm{P}}$ of the form

$$h_0 \sim h_{000}(r,\phi;T) + Gh_{010}(r,\phi;T,\kappa_{\mathrm{A}}/\kappa_{\mathrm{R}}) + \ldots,$$

$$A_0 \sim A_{000}(T) + GA_{010}(T,\kappa_{\mathrm{A}}/\kappa_{\mathrm{R}}) + \ldots,$$

$$\boldsymbol{U}_{\mathrm{P0}} \sim G\boldsymbol{U}_{\mathrm{P010}}(T,\kappa_{\mathrm{A}}/\kappa_{\mathrm{R}}) + \ldots,$$

valid in the limit as $G \to 0$. Note that $\hat{\boldsymbol{U}} \equiv 0$ since the shape of the drop is stationary in our frame of reference, and $\boldsymbol{U}_{\mathrm{P000}} \equiv 0$, a characteristic of the (000)-mode.

Substituting the above expansions into (2.15) gives

$$\nabla_{\mathrm{H}}^2 h_{010} - Th_{010} = -r\cos\phi + A_{010}. \tag{3.1}$$

The expansion of the contact-angle boundary condition (2.14) is more involved because it is evaluated at the contact line, denoted by $r = R_0(\phi;G,0,T)$, whose location is part of the solution. Using a technique common to problems of this sort, an expansion is performed in both the dependent variable and location of the contact line. It is assumed that

$$R_0 \sim R_{000}(\phi;T,\kappa_{\mathrm{A}}/\kappa_{\mathrm{R}}) + GR_{010}(\phi;T,\kappa_{\mathrm{A}}/\kappa_{\mathrm{R}}) + \ldots, \tag{3.2}$$

valid as $G \to 0$, where it has been determined in § 2.3 that $R_{000}(\phi;T) \equiv 1$. Since the location of the contact line is given by $h_0(r,\phi;G,\epsilon,T) = 0$, the expansions for h_0 and R_0 must be related. It is easily shown that

$$h_{000}(1,\phi;T,\kappa_{\mathrm{A}}/\kappa_{\mathrm{R}}) = 0 \quad \text{on} \quad r = 1,$$

$$R_{010} = \frac{-h_{010}}{\partial h_{000}/\partial r} \quad \text{on} \quad r = 1. \tag{3.3}$$

The former expression is used when analysing the (000)-mode (see (2.16)), while the latter is used directly in the expansion of (2.14) to obtain

$$-\kappa(\phi)\, U_{\mathrm{P010}} \cos\phi = \frac{T^{\frac{1}{2}}[I_0(T^{\frac{1}{2}}) + I_2(T^{\frac{1}{2}})]}{2I_1(T^{\frac{1}{2}})} h_{010} - \frac{\partial h_{010}}{\partial r} \quad \text{on} \quad r = 1, \tag{3.4}$$

where

$$\kappa(\phi) \equiv \begin{cases} 1 & \text{for} \quad -\frac{1}{2}\pi < \phi < \frac{1}{2}\pi, \\ \kappa_{\mathrm{A}}/\kappa_{\mathrm{R}} & \text{for} \quad \frac{1}{2}\pi < \phi < \frac{3}{2}\pi. \end{cases}$$

The lowest-order term appearing in the expansion of (2.14) is (2.18). The above expansion assumes that the origin is chosen so that $y = 0$ is the plane of symmetry, and the advancing and receding portions of the contact line are given by $-\frac{1}{2}\pi < \phi < \frac{1}{2}\pi$ and $\frac{1}{2}\pi < \phi < \frac{3}{2}\pi$ respectively. Since the plate is moving in the $-\boldsymbol{i}$-direction, it is anticipated that $U_{\mathrm{P010}} < 0$ (recall that $\boldsymbol{U}_{\mathrm{P}} = U_{\mathrm{P}}\boldsymbol{i}$). The remainder of this section is devoted to obtaining the solution for h_{010}, A_{010} and U_{P010}.

3.2. *Solution*

Let us introduce the variable

$$H_{010} \equiv h_{010} + \frac{A_{010}}{T} - \frac{r\cos\phi}{T}. \tag{3.5}$$

Substituting the above into (3.1) and (3.4) gives

$$\frac{1}{r}\frac{\partial}{\partial r}\left(r\frac{\partial H_{010}}{\partial r}\right) + \frac{1}{r^2}\frac{\partial^2 H_{010}}{\partial \phi^2} - TH_{010} = 0, \tag{3.6}$$

$$T^{\frac{1}{2}}\frac{[I_0(T^{\frac{1}{2}})+I_2(T^{\frac{1}{2}})]}{2I_1(T^{\frac{1}{2}})}H_{010}-\frac{\partial H_{010}}{\partial r}$$
$$=\frac{I_0(T^{\frac{1}{2}})+I_2(T^{\frac{1}{2}})}{2I_1(T^{\frac{1}{2}})}\frac{A_{010}}{T^{\frac{1}{2}}}+\left\{-\kappa(\phi)\,U_{\mathrm{P}010}+\frac{1}{T}-\frac{I_0(T^{\frac{1}{2}})+I_2(T^{\frac{1}{2}})}{2T^{\frac{1}{2}}I_1(T^{\frac{1}{2}})}\right\}\cos\phi \quad \text{on} \quad r=1. \tag{3.7}$$

The inhomogeneity is now relegated to the boundary condition.

It is easily established that a solution to (3.6) is given by

$$H_{010}=G_0\,I_0(rT^{\frac{1}{2}})+\sum_{l=1}^{\infty}I_l(rT^{\frac{1}{2}})\,[F_l\sin l\phi+G_l\cos l\phi], \tag{3.8}$$

where the constants G_0, $\{G_l, F_l : l=1,2,\ldots\}$, A_{010} and $U_{\mathrm{P}010}$ are yet to be determined.

Expanding the function $\kappa(\phi)\cos\phi$ in terms of the basis

$$\{1,\ \sin n\phi,\ \cos n\phi : n=1,2,\ldots\}$$

gives

$$\kappa(\phi)\cos\phi=\frac{1}{\pi}\left(1-\frac{\kappa_{\mathrm{A}}}{\kappa_{\mathrm{R}}}\right)+\frac{1}{2}\left(1+\frac{\kappa_{\mathrm{A}}}{\kappa_{\mathrm{R}}}\right)\cos\phi+\sum_{n=1}^{\infty}\frac{2(-1)^{n+1}(1-\kappa_{\mathrm{A}}/\kappa_{\mathrm{R}})}{\pi(2n-1)\,(2n+1)}\cos 2n\phi. \tag{3.9}$$

Substituting (3.8) and (3.9) into (3.7), and equating coefficients of each like vector of the basis gives the following results:

$$U_{\mathrm{P}010}=\frac{2}{1+\kappa_{\mathrm{A}}/\kappa_{\mathrm{R}}}\left(\frac{2}{T}-\frac{I_0(T^{\frac{1}{2}})}{T^{\frac{1}{2}}I_1(T^{\frac{1}{2}})}\right),$$

$$G_0=\frac{\dfrac{-2U_{\mathrm{P}010}[1-\kappa_{\mathrm{A}}/\kappa_{\mathrm{R}}]}{\pi T^{\frac{1}{2}}I_0(T^{\frac{1}{2}})}+\dfrac{A_{010}[I_0(T^{\frac{1}{2}})+I_2(T^{\frac{1}{2}})]}{TI_0(T^{\frac{1}{2}})\,I_1(T^{\frac{1}{2}})}}{\dfrac{I_0(T^{\frac{1}{2}})+I_2(T^{\frac{1}{2}})}{I_1(T^{\frac{1}{2}})}-\dfrac{2I_1(T^{\frac{1}{2}})}{I_0(T^{\frac{1}{2}})}}, \tag{3.10}$$

$$F_n=0 \quad \text{for} \quad n=1,2,\ldots,$$

$$G_n=\begin{cases}\dfrac{4(-1)^{\frac{1}{2}n}\,(1-\kappa_{\mathrm{A}}/\kappa_{\mathrm{R}})\,U_{\mathrm{P}010}}{\pi(n^2-1)\,T^{\frac{1}{2}}I_n(T^{\frac{1}{2}})\left[\dfrac{I_0(T^{\frac{1}{2}})+I_2(T^{\frac{1}{2}})}{I_1(T^{\frac{1}{2}})}-\dfrac{I_{n-1}(T^{\frac{1}{2}})+I_{n+1}(T^{\frac{1}{2}})}{I_n(T^{\frac{1}{2}})}\right]} & \text{for} \quad n=2,4,\ldots,\\ 0 \quad \text{for} \quad n=3,5,\ldots.\end{cases}$$

Substituting (2.21) into the expression for $U_{\mathrm{P}010}$ gives a somewhat simpler form

$$U_{\mathrm{P}010}=\frac{-2}{(1+\kappa_{\mathrm{A}}/\kappa_{\mathrm{R}})}\frac{V}{\pi a^3\theta_{\mathrm{A}}}. \tag{3.11}$$

The constants G_1 and A_{010} must still be determined.

Recall that (3.4), and hence (3.7), assumes the contact line is advancing, or receding, when $-\frac{1}{2}\pi<\phi<\frac{1}{2}\pi$ or $\frac{1}{2}\pi<\phi<\frac{3}{2}\pi$. This implies that the $x=0$ plane intersects the contact line at its widest point. Assuming that the tangent to the contact line is a continuous function, it is necessary that $\mathrm{d}(R_0\sin\phi)/\mathrm{d}\phi=0$ at $\phi=\pm\frac{1}{2}\pi$. Substituting (3.3), (2.18), (3.5) and (3.8) into (3.2) gives

$$R_0=1+G\left[-\frac{A_{010}}{T}+G_0\,I_0\,(T^{\frac{1}{2}})+\frac{\cos\phi}{T}+\sum_{l=1}^{\infty}G_l\,I_l\,(T^{\frac{1}{2}})\cos l\phi\right].$$

It is easily seen that the above restriction at $\phi=\pm\frac{1}{2}\pi$ gives

$$G_1=\frac{-1}{TI_1(T^{\frac{1}{2}})}.$$

Finally the constant A_{010} is determined by the volume constraint expressed by (2.11). Upon substituting the expansion for h_0 directly into the integrand, and the expansion for R_0 into the limits of integration, it follows that

$$0 = \int_0^{2\pi} \int_0^1 h_{010} r \, \mathrm{d}r \, \mathrm{d}\phi.$$

Evaluating the above using the solution for h_{010} thus far derived gives

$$G_0 I_1(T^{\frac{1}{2}}) - \frac{A_{010}}{2T^{\frac{1}{2}}} = 0.$$

Combining the above with (3.10) gives

$$A_{010} = \frac{\dfrac{4U_{\mathrm{P}010}}{\pi} \dfrac{I_1(T^{\frac{1}{2}})}{I_2(T^{\frac{1}{2}})} \left(1 - \dfrac{\kappa_{\mathrm{A}}}{\kappa_{\mathrm{R}}}\right)}{\dfrac{2I_1(T^{\frac{1}{2}})}{I_2(T^{\frac{1}{2}})} - \dfrac{I_0(T^{\frac{1}{2}}) + I_2(T^{\frac{1}{2}})}{I_1(T^{\frac{1}{2}})}}.$$

4. The critical static configuration of a drop on an inclined plane with contact-angle hysteresis

4.1. *Formulation of boundary-value problem*

For a given material system, i.e. ϵ is specified, a drop will move down any surface inclined at any $\gamma > \gamma_{\mathrm{c}}$, where $\gamma_{\mathrm{c}} = \gamma_{\mathrm{c}}(\epsilon)$. Its shape when $\gamma = \gamma_{\mathrm{c}}$ is determined by examining the limit as $U_{\mathrm{D}} \to 0$, $U_{\mathrm{D}} > 0$ (see figure 4). In this limit, the contact angle must be θ_{A} along the lower portion of the contact line, and θ_{R} along the upper portion. The boundary-value problem, expressed in terms of parameters G and T, is

$$\nabla_{\mathrm{H}}^2 h_{0\mathrm{c}} - T h_{0\mathrm{c}} = -G_{\mathrm{c}} x + A_{0\mathrm{c}}, \tag{4.1}$$

with

$$\left.\begin{aligned} |\nabla_{\mathrm{H}} h_{0\mathrm{c}}| = \begin{cases} 1 & \text{for } -\phi_{\mathrm{A}0\mathrm{c}} < \phi < \phi_{\mathrm{A}0\mathrm{c}}, \\ 1-\epsilon & \text{for } \phi_{\mathrm{R}0\mathrm{c}} < \phi < 2\pi - \phi_{\mathrm{R}0\mathrm{c}}, \end{cases} \\ \text{contact line is a straight-line segment} \quad \begin{cases} \phi_{\mathrm{A}0\mathrm{c}} < \phi < \phi_{\mathrm{R}0\mathrm{c}} \\ 2\pi - \phi_{\mathrm{R}0\mathrm{c}} < \phi < 2\pi - \phi_{\mathrm{A}0\mathrm{c}}, \end{cases} \end{aligned}\right\} \tag{4.2}$$

$$\int_S h_{0\mathrm{c}} \, \mathrm{d}s = \frac{V}{a^3 \theta_{\mathrm{A}}}, \tag{4.3}$$

where

$$\left.\begin{aligned} z &= h_{0\mathrm{c}}(r, \gamma; G_{\mathrm{c}}, \epsilon, T), \\ A_{0\mathrm{c}} &= A_{0\mathrm{c}}(G_{\mathrm{c}}, \epsilon, T), \\ \gamma_{\mathrm{A}0\mathrm{c}} &= \gamma_{\mathrm{A}0\mathrm{c}}(G_{\mathrm{c}}, \epsilon, T), \\ \gamma_{\mathrm{R}0\mathrm{c}} &= \gamma_{\mathrm{R}0\mathrm{c}}(G_{\mathrm{c}}, \epsilon, T), \\ G_{\mathrm{c}} &= G_{\mathrm{c}}(\epsilon, T) \end{aligned}\right\} \tag{4.4}$$

must all be determined. Since a specific static configuration is sought, the subscript c is included.

It can be anticipated that a perturbation solution to the above problem, valid for $\epsilon \to 0$, is singular. This is a direct consequence of the fact that when $\epsilon \equiv 0$ no straight-line segments need be present in the contact line at the sides of the drop, while they must be present for $\epsilon \not\equiv 0$, no matter how small its value. In § 4.2 a solution

is obtained for the lowest-order modes in the outer region. The inner region, i.e. the region in the immediate vicinity of the straight-line segments, is analysed in §4.3. Three restrictions are placed on the inner solution in §4.4 so that it is acceptable from a physical point of view, and in §4.5 the inner and outer solutions are matched.

4.2. *Outer region*

The appropriate scales for the outer region are the same as those already introduced in §2.2. Expansion in ϵ of the quantities identified in (4.4) are assumed of the forms

$$h_{0c} \sim h_{000}(r,\phi;T)+\epsilon\ln\epsilon\, h_{0cL}(r,\phi;T)+\epsilon h_{0c1}(r,\phi;T)+\ldots, \tag{4.5a}$$

$$A_{0c} \sim A_{000}(T)+\epsilon\ln\epsilon\, A_{0cL}(T)+\epsilon\, A_{0c1}(T)+\ldots, \tag{4.5b}$$

$$\phi_{A0c} \sim \tfrac{1}{2}\pi+\epsilon\phi_{A0c1}(T)+\ldots, \tag{4.5c}$$

$$\phi_{A0c} \sim \tfrac{1}{2}\pi+\epsilon\phi_{R0c1}(T)+\ldots, \tag{4.5d}$$

$$G_c \sim \epsilon\ln\epsilon\, G_{cL}(T)+\epsilon G_{c1}(T)+\ldots, \tag{4.5e}$$

valid in the limit as $\epsilon\to 0$. The necessity to include terms proportional to $\epsilon\ln\epsilon$ in the expansions of h_{0c}, A_{0c} and G_c becomes evident when matching (see §4.5). They do not appear in the expansions of ϕ_{A0c} and ϕ_{R0c} because the scale of the size of the inner region is ϵ. The lowest-order mode (000) has already been solved in §2.3.

We begin by solving the (0C1) mode. Substituting the above expansions into (4.1)–(4.3) gives

$$\nabla_H^2 h_{0c1} - T h_{0c1} = -G_{c1}x + A_{0c1}, \tag{4.6}$$

$$\frac{T^{\frac{1}{2}}[I_0(T^{\frac{1}{2}})+I_2(T^{\frac{1}{2}})]}{2I_1(T^{\frac{1}{2}})}h_{0c1} - \frac{\partial h_{0c1}}{\partial r} = \begin{cases} 0 & \text{for } \tfrac{1}{2}\pi<\phi<\tfrac{1}{2}\pi, \quad r=1, \\ -1 & \text{for } \tfrac{1}{2}\pi<\phi<\tfrac{3}{2}\pi, \quad r=1, \end{cases} \tag{4.7}$$

$$\int_0^{2\pi}\int_0^1 h_{0c1}\, r\,\mathrm{d}r\,\mathrm{d}\phi = 0, \tag{4.8}$$

where the contact-angle boundary condition and the volume constraint have been expanded in a manner similar to that described in §3.1. Singularities can be anticipated at $\phi = \pm\frac{1}{2}\pi$ due to the discontinuities in the function on the right-hand side of (4.7).

The solution is obtained by using the same procedure presented in §3.2. Equation (4.6) is made homogeneous by introducing a new dependent variable

$$H_{0c1} \equiv h_{0c1} + \frac{A_{0c1}}{T} - \frac{G_{c1}}{T} r\cos\phi. \tag{4.9}$$

It is easily shown that a solution for H_{0c1} can be represented by

$$H_{0c1} = B_0\, I_0(rT^{\frac{1}{2}}) + \sum_{l=1}^{\infty} B_l\, I_l(rT^{\frac{1}{2}})\cos l\phi. \tag{4.10}$$

Substituting (4.10) and (4.9) into (4.7) and recognizing that

$$-\tfrac{1}{2} + \sum_{n=0}^{\infty}\frac{2(-1)^n}{\pi(2n+1)}\cos(2n+1)\phi = \begin{cases} 0 & \text{for } -\tfrac{1}{2}\pi<\phi<\tfrac{1}{2}\pi, \\ -1 & \text{for } \tfrac{1}{2}\pi<\phi<\tfrac{3}{2}\pi \end{cases}$$

gives the following:

$$G_{c1} = \frac{2T^{\frac{1}{2}}I_1(T^{\frac{1}{2}})}{\pi I_2(T^{\frac{1}{2}})}, \tag{4.11}$$

$$B_0 = \frac{-T^{\frac{1}{2}}I_1(T^{\frac{1}{2}}) + A_{0c1}[I_0(T^{\frac{1}{2}}) + I_2(T^{\frac{1}{2}})]}{TI_0(T^{\frac{1}{2}})\,[I_0(T^{\frac{1}{2}}) + I_2(T^{\frac{1}{2}})] - 2T[I_1(T^{\frac{1}{2}})]^2}, \tag{4.12}$$

$$B_{2n+1} = \frac{\dfrac{4(-1)^n}{\pi T^{\frac{1}{2}}(2n+1)}}{\left[\dfrac{I_0(T^{\frac{1}{2}}) + I_2(T^{\frac{1}{2}})}{I_1(T^{\frac{1}{2}})}\right] I_{2n+1}(T^{\frac{1}{2}}) - [I_{2n}(T^{\frac{1}{2}}) + I_{2n+2}(T^{\frac{1}{2}})]} \quad \text{for} \quad n = 1, 2, 3, \ldots, \tag{4.13}$$

$$B_{2n} = 0 \quad \text{for} \quad n = 1, 2, \ldots. \tag{4.14}$$

The constant A_{0c1} is determined by (4.8), which becomes

$$B_0 I_1(T^{\frac{1}{2}}) - \frac{A_{0c1}}{2T^{\frac{1}{2}}} = 0,$$

and (4.12) to give

$$A_{0c1} = \frac{-2[I_1(T^{\frac{1}{2}})]^2}{[I_0(T^{\frac{1}{2}}) + I_2(T^{\frac{1}{2}})]\, I_2(T^{\frac{1}{2}}) - 2[I_1(T^{\frac{1}{2}})]^2}. \tag{4.15}$$

The constant B_1 is yet to be determined.

It is natural to proceed in a similar fashion as that outlined in §3.2 to calculate B_1. It can easily be shown that $R_{0c1} = h_{0c1}(1, \phi; T)$, where an explicit representation of the location of the contact line is given by

$$R_{0c} \sim 1 + \epsilon \ln \epsilon\, R_{0cL}(\phi; T) + \epsilon R_{0c1}(\phi; T) + \ldots.$$

Substituting (4.9), (4.10) and (4.14) into the above gives

$$R_{0c} \sim 1 + \epsilon \ln \epsilon\, R_{0cL} + \epsilon\left[-\frac{A_{0c1}}{T} + B_0 I_0(T^{\frac{1}{2}}) + \left[\frac{G_{c1}}{T} + B_1 I_1(T^{\frac{1}{2}})\right]\cos\phi + \sum_{n=1}^{\infty} B_{2n+1} I_{2n+1}(T^{\frac{1}{2}}) \cos(2n+1)\phi\right]. \tag{4.16}$$

However, (4.7) requires that the maximum width of the drop lies in the $x = 0$ plane; i.e. $\mathrm{d}(R_{0c} \sin\phi)/\mathrm{d}\phi = 0$ at $\phi = \pm\frac{1}{2}\pi$, which implies

$$\frac{\mathrm{d}R_{0c1}}{\mathrm{d}\phi} = 0 \quad \text{at} \quad \phi = \pm\tfrac{1}{2}\pi. \tag{4.17}$$

But it can be shown that $R_{0c1} \sim O(x \ln |x|)$ as $x \to 0$ (refer to §4.5), hence $|\mathrm{d}R_{0c1}/\mathrm{d}\phi| \to \infty$ as $\phi \to \pm\frac{1}{2}\pi$. No finite value of B_1 can be chosen so that (4.17) is satisfied. Thus the solution is singular in the neighbourhood of $(1, \frac{1}{2}\pi)$ and $(1, -\frac{1}{2}\pi)$. A different expansion in ϵ must be used in order to obtain a solution valid in these regions. This is pursued in §4.3.

In the remainder of this subsection a solution to the (OCL) mode is determined. It is easily shown that the boundary-value problem is

$$\left.\begin{aligned} \nabla^2 h_{0cL} - T h_{0cL} &= A_{0cL} - G_{0cL}\, x, \\ \frac{T^{\frac{1}{2}}[I_0(T^{\frac{1}{2}}) + I_2(T^{\frac{1}{2}})]}{2I_1(T^{\frac{1}{2}})} h_{0cL} - \frac{\partial h_{0cL}}{\partial r} &= 0 \quad \text{on} \quad r = 1, \\ \int_0^{2\pi}\int_0^1 h_{0cL}\, r\, \mathrm{d}r\, \mathrm{d}\phi &= 0. \end{aligned}\right\} \tag{4.18}$$

The solution for h_{0cL} is obtained in an identical manner as for h_{0c1}. It is straightforward to show that

$$h_{0cL} = \frac{A_{0cL}}{T}\left\{\frac{[I_0(T^{\frac{1}{2}})+I_2(T^{\frac{1}{2}})][I_0(rT^{\frac{1}{2}})-I_0(T^{\frac{1}{2}})]+2[I_1(T^{\frac{1}{2}})]^2}{I_0(T^{\frac{1}{2}})[I_0(T^{\frac{1}{2}})+I_2(T^{\frac{1}{2}})]-2[I_1(T^{\frac{1}{2}})]^2}\right\} + L_1 I_1(rT^{\frac{1}{2}})\cos\phi,$$

$$G_{cL} = 0,$$

and

$$R_{0cL} = \frac{2A_{0cL}[I_1(T^{\frac{1}{2}})]^2}{TI_0(T^{\frac{1}{2}})[I_0(T^{\frac{1}{2}})+I_2(T^{\frac{1}{2}})]-2T[I_1(T^{\frac{1}{2}})]^2} L_1 I_1(T^{\frac{1}{2}})\cos\phi.$$

Equation (4.18) gives $A_{0cL} = 0$; hence the solution of the (0cL) mode is

$$h_{0cL} = L_1 I_1(r, T^{\frac{1}{2}})\cos\phi,$$

$$R_{0cL} = L_1 I_1(T^{\frac{1}{2}})\cos\phi,$$

where the constant L_1 is yet to be determined.

4.3. *Inner region*

The two inner regions located in the neighbourhood of $(1, \frac{1}{2}\pi)$ and $(1, -\frac{1}{2}\pi)$ are identical in nature since the problem is symmetric about the $y = 0$ plane. Therefore we need only analyse the solution near $(1, \frac{1}{2}\pi)$. It is convenient to introduce a new rectangular cartesian coordinate system $(\bar{x}, \bar{y})$ defined by

$$\bar{x} \equiv -x, \quad \bar{y} \equiv 1-y.$$

The scale of the inner region can be anticipated by (4.2) to be ϵ, thus introducing the inner independent and dependent variables

$$\bar{x}_\epsilon \equiv \frac{\bar{x}}{\epsilon}, \quad \bar{y}_\epsilon \equiv \frac{\bar{y}}{\epsilon}, \quad \bar{z}_\epsilon \equiv \frac{\bar{z}}{\epsilon}, \quad h_{\epsilon 0c} \equiv \frac{h_{0c}}{\epsilon}.$$

The justification of this choice is based on the successful matching of the solutions in the inner and outer regions (§4.5). The straight-line segments of the contact line on the side of the drop lie within the inner region, with endpoints located at $\bar{x}_\epsilon = \pm L_\epsilon$ (see figure 5). Thus, their length in dimensional form is given by $2\epsilon a L_\epsilon$, and the location of the $x = 0$ plane is specified.

An asymptotic expansion of $h_{\epsilon 0c}$ is assumed to have the form

$$h_{\epsilon 0c} \sim h_{\epsilon 000}(\bar{x}_\epsilon, \bar{y}_\epsilon; T) + \epsilon h_{\epsilon 0c1}(\bar{x}_\epsilon, \bar{y}_\epsilon; T) + \ldots \tag{4.19}$$

valid in the limit as $\epsilon \to 0$. Expansions for A_{0c}, ϕ_{A0c}, ϕ_{R0c}, and G_c have already been specified by (4.5*b–e*). In fact, all of the leading terms appearing in these expansions have been determined by the outer solution except for ϕ_{A0c1}, ϕ_{R0c1}, and L_1.

The governing equation and boundary condition for the inner region are obtained in the usual way. To lowest order, i.e. $O(1)$ as $\epsilon \to 0$, one finds

$$\frac{\partial^2 h_{\epsilon 000}}{\partial \bar{x}_\epsilon^2} + \frac{\partial^2 h_{\epsilon 000}}{\partial \bar{y}_\epsilon^2} = 0,$$

$$h_{\epsilon 000}(\bar{x}_\epsilon, \bar{y}_\epsilon) = 0,$$

$$\left(\frac{\partial h_{\epsilon 000}}{\partial \bar{x}_\epsilon}\right)^2 + \left(\frac{\partial h_{\epsilon 000}}{\partial \bar{y}_\epsilon}\right)^2 = 1 \quad \text{on} \quad \bar{y}_\epsilon = \bar{Y}_{\epsilon 000}.$$

In the above formulation the location of the contact line is given by $\bar{y}_\epsilon = \bar{Y}_{\epsilon 0c}$, where an expansion has been assumed of the form

$$\bar{Y}_{\epsilon 0c} \sim \bar{Y}_{\epsilon 000}(T) + \epsilon \bar{Y}_{\epsilon 0c1}(\bar{x}_\epsilon; T) + \ldots,$$

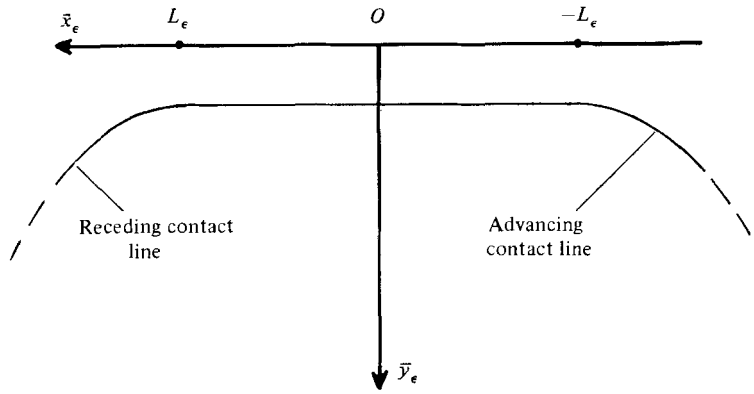

FIGURE 5. The shape of the contact line as viewed from the inner region. The original of the coordinate system $(\bar{x}_\epsilon, \bar{y}_\epsilon)$ is located midway between the ends of the straight-line segments and a distance of 1 from the centre of the drop.

valid in the limit as $\epsilon \to 0$. Note that the contact line is being expanded about the straight line $\overline{Y}_\epsilon = \overline{Y}_{\epsilon 000}$, whose location is yet to be determined. This differs to $O(\epsilon)$ as $\epsilon \to 0$ from the location at which the outer representation of the contact line has been expanded about in the neighbourhood of $\phi = \frac{1}{2}\pi$. The solution to the above boundary-value problem is

$$h_{\epsilon 000} = \bar{y}_\epsilon - \overline{Y}_{\epsilon 000}. \tag{4.20}$$

The boundary-value problem to $O(\epsilon)$ as $\epsilon \to 0$ is

$$\frac{\partial^2 h_{\epsilon 0c1}}{\partial \bar{x}_\epsilon^2} + \frac{\partial^2 h_{\epsilon 0c1}}{\partial \bar{y}_\epsilon^2} = A_{000},$$

$$h_{\epsilon 0c1} = -\overline{Y}_{\epsilon 0c1} \quad \text{on} \quad \bar{y}_\epsilon = \overline{Y}_{\epsilon 000} \quad \text{for} \quad -L_\epsilon < \bar{x}_\epsilon < L_\epsilon,$$

$$\frac{\partial h_{\epsilon 0c1}}{\partial \bar{y}_\epsilon} = \begin{cases} 0 & \text{on} \quad \bar{y}_\epsilon = \overline{Y}_{\epsilon 000} \quad \text{for} \quad \bar{x}_\epsilon < -L_\epsilon, \\ -1 & \text{on} \quad \bar{y}_\epsilon = \overline{Y}_{\epsilon 000} \quad \text{for} \quad \bar{x}_\epsilon > L_\epsilon, \end{cases}$$

where the value of A_{000} is given by (2.20). Note that if we introduce the variable w_{0c}, the width of the drop made dimensionless with a, then its expansion in ϵ is

$$w_{0c} \sim 2 + \epsilon w_{0c1} + \epsilon^2 w_{0c2} + \ldots,$$

valid as $\epsilon \to 0$. However, $w_{0c} \equiv 2 - 2\epsilon \overline{Y}_{\epsilon 0c}(0; T, \epsilon)$. Hence we can make the identification that

$$w_{0c1} = -2\overline{Y}_{\epsilon 000}, \quad w_{0c2} = -2\overline{Y}_{\epsilon 0c1}.$$

The remainder of this subsection is devoted to obtaining the solution to the above problem.

As with previous problems, we begin by defining a new dependent variable, $H_{\epsilon 0c1}$ so that the only inhomogeneous term in the boundary-value problem appears in the boundary conditions

$$H_{\epsilon 0c1} \equiv h_{\epsilon 0c1} - \tfrac{1}{2}\bar{x}_\epsilon^2 A_{000}. \tag{4.21}$$

In obtaining a solution for $H_{\epsilon 0c1}$ it is convenient to write

$$H_{\epsilon 0c1} = H_\infty + H_R,$$

where H_∞ satisfies

$$\frac{\partial^2 H_\infty}{\partial \bar{x}_\epsilon^2} + \frac{\partial^2 H_\infty}{\partial \bar{y}_\epsilon^2} = 0, \tag{4.22}$$

$$\frac{\partial H_\infty}{\partial \bar{y}_\epsilon} = \begin{cases} 0 & \text{on} \quad \bar{y}_\epsilon = \overline{Y}_{000} \quad \text{for} \quad \bar{x}_\epsilon < 0, \\ -1 & \text{on} \quad \bar{y}_\epsilon = \overline{Y}_{\epsilon 000} \quad \text{for} \quad \bar{x}_\epsilon > 0, \end{cases} \tag{4.23}$$

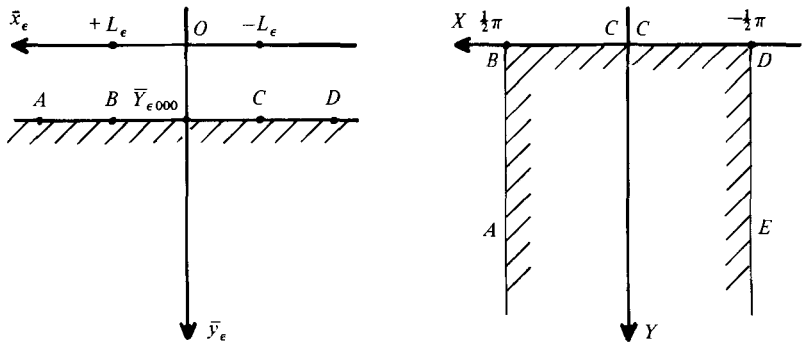

(*a*) (*b*)

FIGURE 6. The shaded areas in (*a*) and (*b*) indicate the domain over which a solution is sought. The locations of the points A, B, C, D and E indicate the transformation of the boundary.

It can easily be shown that a particular solution is

$$H_\infty = -(\bar{y}_\epsilon - \bar{\bar{Y}}_{\epsilon 000})\left(\tfrac{1}{2} + \frac{1}{\pi}\tan^{-1}\frac{\bar{x}_\epsilon}{\bar{y}_\epsilon - \bar{\bar{Y}}_{\epsilon 000}}\right) - \frac{\bar{x}_\epsilon}{2\pi}\ln\left[\bar{x}_\epsilon^2 + (\bar{y}_\epsilon - \bar{\bar{Y}}_{\epsilon 000})^2\right] + \frac{\bar{x}_\epsilon}{\pi}. \quad (4.24)$$

Thus H_{R} must satisfy

$$\frac{\partial^2 H_{\mathrm{R}}}{\partial \bar{x}_\epsilon^2} + \frac{\partial^2 H_{\mathrm{R}}}{\partial \bar{y}_\epsilon^2} = 0,$$

$$\frac{\partial H_{\mathrm{R}}}{\partial \bar{y}_\epsilon} = 0 \quad \text{on} \quad \bar{y}_\epsilon = \bar{\bar{Y}}_{\epsilon 000} \quad \text{for} \quad |\bar{x}_\epsilon| > L_\epsilon,$$

$$H_{\mathrm{R}} = \frac{w_{0c2}}{2} - \frac{\bar{x}_\epsilon^2}{2}A_{000} + \frac{\bar{x}_\epsilon}{2\pi}\ln\bar{x}_\epsilon^2 - \frac{\bar{x}_\epsilon}{\pi} \quad \text{on} \quad \bar{y}_\epsilon = \bar{\bar{Y}}_{\epsilon 000} \quad \text{for} \quad -L_\epsilon < \bar{x}_\epsilon < L_\epsilon.$$

The boundary-value problem defined above has a mixed boundary condition along $\bar{y}_\epsilon = \bar{\bar{Y}}_{\epsilon 000}$ since it is of the first kind over the interval $-L_\epsilon < \bar{x}_\epsilon < L_\epsilon$, and of the second kind over $|\bar{x}_\epsilon| > L_\epsilon$. In order to reduce the problem to a more typical form, the coordinates are transformed from $(\bar{x}_\epsilon, \bar{y}_\epsilon)$ to (X, Y) by

$$\frac{\bar{x}_\epsilon}{L_\epsilon} = \cosh Y \sin X, \quad \frac{\bar{y}_\epsilon - \bar{\bar{Y}}_{\epsilon 000}}{L_\epsilon} = \sinh Y \cos X.$$

This maps the semi-infinite plane

$$\{(\bar{x}_\epsilon, \bar{y}_\epsilon) | \bar{y}_\epsilon \geqslant \bar{\bar{Y}}_{\epsilon 000};\ -\infty < \bar{x}_\epsilon < \infty\}$$

over which a solution is sought into the semi-infinite strip

$$\{(X, Y) | Y \geqslant 0;\ -\tfrac{1}{2}\pi \leqslant X \leqslant \tfrac{1}{2}\pi\}$$

(see figure 6). The boundary-value problem transforms to

$$\frac{\partial^2 H_{\mathrm{R}}}{\partial X^2} + \frac{\partial^2 H_{\mathrm{R}}}{\partial Y^2} = 0, \quad (4.25)$$

$$\frac{\partial H_{\mathrm{R}}}{\partial X} = 0 \quad \text{on} \quad Y > 0 \quad \text{for} \quad X = \pm\tfrac{1}{2}\pi, \quad (4.26)$$

$$H_{\mathrm{R}} = \frac{w_{0c2}}{2} - \frac{L_\epsilon^2}{2}A_{000}\sin^2 X + \frac{L_\epsilon}{\pi}\sin X \ln\left(L_\epsilon^2 \sin^2 X\right) - \frac{L_\epsilon}{\pi}\sin X$$

$$\text{on} \quad Y = 0 \quad \text{for} \quad -\tfrac{1}{2}\pi < X < \tfrac{1}{2}\pi. \quad (4.27)$$

It is easily shown that a solution to (4.25) and (4.26) is

$$H_{\mathrm{R}} = C_0\, Y + D_0 + \sum_{k=0}^{\infty} [C_{2k+1} \mathrm{e}^{(2k+1)\,Y} + D_{2k+1} \mathrm{e}^{-(2k+1)\,Y}] \sin{(2k+1)\,X} + \sum_{k=1}^{\infty} [C_{2k} \mathrm{e}^{2kY} + D_{2k} \mathrm{e}^{-2kY}] \cos{2kX}. \quad (4.28)$$

To determine the unknown constants, we begin by noting that

$$\sin X \ln(\sin^2 X) = (1 - 2\ln 2) \sin X + \sum_{k=1}^{\infty} \left(\frac{1}{k+1} - \frac{1}{k}\right) \sin{(2k+1)\,X},$$

and that

$$\sin^2 X = \tfrac{1}{2} - \tfrac{1}{2} \cos 2X.$$

Substituting the above two relationships into (4.27) and (4.28) gives the following:

$$D_0 = \tfrac{1}{2} w_{0c2} - \tfrac{1}{4} L_\epsilon^2 A_{000}, \quad C_1 + D_1 = \frac{L_\epsilon}{2\pi}\left(-1 + \ln \frac{L_\epsilon^2}{4}\right),$$

$$C_2 + D_2 = L_\epsilon^2 \frac{A_{000}}{4}, \quad \left\{C_{2k+1} + D_{2k+1} = \frac{L_\epsilon}{2\pi}\left(\frac{1}{k+1} - \frac{1}{k}\right) : k = 1, 2, \ldots\right\}.$$

Substituting the above into (4.28) and adding (4.24) gives

$$\begin{aligned} H_{\epsilon 0 c 1} = {} & -L_\epsilon \left[\frac{1}{2} + \frac{1}{\pi} \tan^{-1} \frac{\cosh Y \sin X}{\sinh Y \cos X}\right] \sinh Y \cos X + C_0\, Y + \tfrac{1}{2} w_{0c2} \\ & - \frac{L_\epsilon}{2\pi} [\ln L_\epsilon^2 - 2 + \ln(\cosh^2 Y \sin^2 X + \sinh^2 Y \cos^2 X)] \cosh Y \sin X \\ & - \tfrac{1}{4} L_\epsilon^2 A_{000} + \frac{L_\epsilon}{2\pi} (-1 + \ln \tfrac{1}{4} L_\epsilon^2) \mathrm{e}^{-Y} \sin X + C_1 \sinh Y \sin X \\ & + \tfrac{1}{4} L_\epsilon^2 A_{000} \mathrm{e}^{-2Y} \cos 2X + 2C_2 \sinh 2Y \cos 2X \\ & + \sum_{k=1}^{\infty} 2C_{2k+1} \sinh{(2k+1)\,Y} \sin{(2k+1)\,X} \\ & - \frac{L_\epsilon}{2\pi} \mathrm{e}^{-Y} \sin X + \frac{L_\epsilon}{\pi} \cos X \sinh Y \tan^{-1} \frac{\mathrm{e}^{-2Y} \sin 2X}{1 - \mathrm{e}^{-2Y} \cos 2X} \\ & + \frac{L_\epsilon}{\pi} \sin X \cosh Y \ln(1 - 2\mathrm{e}^{-2Y} \cos 2X + \mathrm{e}^{-4Y})^{\frac{1}{2}}, \end{aligned} \quad (4.29)$$

where the constants $w_{0c2}, L_\epsilon, C_0, C_2$, and $\{C_{2k+1} : k = 0, 1, 2, \ldots\}$ are as yet undetermined. It should be noted that the following identity was used in deriving (4.29):

$$\begin{aligned} \sum_{k=1}^{\infty} \left[\frac{1}{k+1} - \frac{1}{k}\right] \mathrm{e}^{-(2k+1)\,Y} \sin{(2k+1)\,X} & \\ = -\mathrm{e}^{-Y} \sin X + 2 \cos X \sinh Y \tan^{-1} \frac{\mathrm{e}^{-2Y} \sin 2X}{1 - \mathrm{e}^{-2Y} \cos 2X} & \\ + 2 \sin X \cosh Y \ln(1 - \mathrm{e}^{-2Y} \cos 2X + \mathrm{e}^{-4Y})^{\frac{1}{2}}. & \end{aligned} \quad (4.30)$$

Before proceeding to match the inner and outer solutions, there remain three additional restrictions that must be satisfied by the inner solution. These are presented in §4.4.

4.4. *Compatibility conditions on the solution within the inner region*

Three additional conditions must be satisfied by the inner solution in order for it to be acceptable from a physical point of view. Even though the contact angle is not specified along the straight-line segments, it has been established in §2.1 that its value must lie within the interval $[\theta_R, \theta_A]$. The second condition arises from the fact that the solution in the neighbourhood of the endpoints of the straight-line segments must be consistent with the small-slope approximation. It is shown below that the consequence of this requirement is a continuous tangent along the contact line. The third condition reflects the fact that the drop is widest between the straight-line segments. Since the second condition results in $\mathrm{d}\bar{Y}_{\epsilon 0c}/\mathrm{d}\bar{x}_\epsilon = 0$ at $\bar{x}_\epsilon = \pm L_\epsilon$, this last condition requires $\mathrm{d}^2\bar{Y}_{\epsilon 0c}/\mathrm{d}\bar{x}_\epsilon^2 \geqslant 0$ as $\bar{x}_\epsilon \to \pm L_\epsilon$ for $|\bar{x}_\epsilon| > L_\epsilon$.

It is easily shown that the first condition mentioned above implies

$$-1 \leqslant \frac{\partial h_{\epsilon 0c1}}{\partial \bar{y}_\epsilon} \leqslant 0 \quad \text{on} \quad \bar{y}_\epsilon = \bar{Y}_{\epsilon 000} \quad \text{for} \quad -L_\epsilon \leqslant \bar{x}_\epsilon \leqslant L_\epsilon. \tag{4.31}$$

Taking into account the various changes in variable, one finds

$$\left.\frac{\partial h_{\epsilon 0c1}}{\partial \bar{y}_\epsilon}\right|_{\bar{y}_\epsilon = \bar{Y}_{\epsilon 000}} = \frac{1}{L_\epsilon \cos X}\left.\frac{\partial H_{\epsilon 0c1}}{\partial Y}\right|_{Y=0}.$$

The right-hand side of the above equation can be evaluated using (4.30) to give

$$\left.\frac{\partial h_{\epsilon 0c1}}{\partial \bar{y}_\epsilon}\right|_{\bar{y}_\epsilon = \bar{Y}_{\epsilon 000}} = L_\epsilon \cos X - \frac{1}{\pi}(X + \tfrac{1}{2}\pi) \quad \text{for} \quad -\tfrac{1}{2}\pi \leqslant X \leqslant \tfrac{1}{2}\pi.$$

It is straightforward to show that (4.31) implies

$$L_\epsilon \leqslant \frac{1}{\pi}. \tag{4.32}$$

Since the shape of the contact line and the surface of the drop are related to $O(\epsilon)$ as $\epsilon \to 0$ by

$$\bar{Y}_{\epsilon 0c1} = -h_{\epsilon 0c1}(\bar{x}_\epsilon, \bar{Y}_{\epsilon 000}),$$

it follows directly that $|\mathrm{d}\bar{Y}_{\epsilon 0c1}/\mathrm{d}\bar{x}_\epsilon| < \infty$ is necessary for $|\nabla h_{\epsilon 0c1}|$ to be uniformly bounded, a requirement of the small-slope approximation. It is easily shown that along positions corresponding to $|\bar{x}_\epsilon| > L_\epsilon$ one gets

$$-\frac{\mathrm{d}\bar{Y}_{\epsilon 0c1}}{\mathrm{d}\bar{x}_\epsilon} = \frac{\pm 1}{(\bar{x}_\epsilon^2 - L_\epsilon^2)^{\frac{1}{2}}}\left.\frac{\mathrm{d}H_{\epsilon 0c1}}{\mathrm{d}Y}\right|_{(\pm\frac{1}{2}\pi, Y)} + \bar{x}_\epsilon A_{000}. \tag{4.33}$$

Since we are primarily interested in the neighbourhood of $\bar{x}_\epsilon = \pm L_\epsilon$, a Taylor series is performed on $\mathrm{d}H_{\epsilon 0c1}/\mathrm{d}Y|_{(\pm\frac{1}{2}\pi, Y)}$ about $Y = 0$, yielding

$$\begin{aligned}\left.\frac{\mathrm{d}H_{\epsilon 0c1}}{\mathrm{d}Y}\right|_{(\pm\frac{1}{2}\pi, Y)} &= \left[C_0 \pm \frac{L_\epsilon}{\pi}\ln\frac{2}{L_\epsilon} \pm 2C_1 + \frac{L_\epsilon^2}{2}A_{000} - 4C_2\right] - L_\epsilon^2 A_{000}\, Y \\ &\quad + \left[\pm\frac{L_\epsilon}{2\pi}\left(-4 + \ln\frac{4}{L_\epsilon^2}\right) \pm 2C_1 + 2L_\epsilon^2 A_{000} - 16C_2\right]\frac{Y^2}{2} + \ldots,\end{aligned} \tag{4.34}$$

where it has been assumed $\{C_{2k+1} = 0 : k = 1, 2, \ldots\}$, a consequence of matching (see §4.5). It is evident that $|\mathrm{d}\bar{Y}_{\epsilon 0c1}/\mathrm{d}\bar{x}_\epsilon| < \infty$ implies

$$C_0 \pm \frac{L_\epsilon}{\pi}\ln\frac{2}{L_\epsilon} \pm 2C_1 + \tfrac{1}{2}L_\epsilon^2 A_{000} - 4C_2 = 0.$$

These two equations can be rewritten as

$$C_0+\tfrac{1}{2}L_\epsilon^2 A_{000}-4C_2=0, \tag{4.35}$$

$$C_1=\frac{L_\epsilon}{2\pi}\ln\frac{L_\epsilon}{2}. \tag{4.36}$$

It is easily shown that not only are (4.35) and (4.36) necessary for the validity of the small-slope approximation, they also imply that $\mathrm{d}\overline{Y}_{\epsilon 0c1}/\mathrm{d}\bar{x}_\epsilon \to 0$ as $\bar{x}_\epsilon \to \pm L_\epsilon$ for $|\bar{x}_\epsilon| > L_\epsilon$.

In order to impose the third condition, an expression for the curvature of the contact line valid near the endpoints of the straight-line segment is required. Differentiating (4.33) and making use of (4.34)–(4.36) gives

$$\frac{\mathrm{d}^2\overline{Y}_{\epsilon 0c1}}{\mathrm{d}\bar{x}_\epsilon^2}\sim\frac{2C_0\pm L_\epsilon/\pi}{L_\epsilon^2\sqrt{2^{\frac{1}{2}}(|\bar{x}_\epsilon/L_\epsilon|-1)^{\frac{1}{2}}}}-A_{000}\quad\text{as}\quad\bar{x}_\epsilon\to\pm L_\epsilon\quad\text{for}\quad|\bar{x}_\epsilon|>L_\epsilon.$$

The requirement that $\mathrm{d}^2\overline{Y}_{\epsilon 0c1}/\mathrm{d}\bar{x}^2 \geqslant 0$ as $\bar{x}_\epsilon \to \pm L_\epsilon$ for $|\bar{x}_\epsilon| > L_\epsilon$ implies

$$\pm\frac{L_\epsilon}{\pi}\geqslant -2C_0. \tag{4.37}$$

In §4.5 the value of C_0 is determined. Equations (4.32) and (4.37) can then be used to determine L_ϵ.

4.5. *Matching*

The constants L_ϵ, C_0, $\{C_{2k+1}: k=1,2,\ldots\}$, $\overline{Y}_{\epsilon 000}$, L_1 and B_1 are determined by matching the inner and outer solutions. This is accomplished by expressing the solution valid in the inner region in terms of the outer variables $(\bar{x},\bar{y})$ and expanding it in terms of the asymptotic sequence $\{1,\epsilon\ln\epsilon,\epsilon,\ldots\}$. The abovementioned constants are determined by equating this expression to the local form of the outer solution.

The *inner* solution to $O(\epsilon)$ as $\epsilon\to 0$ is obtained by combining (4.21), (4.29), (4.19) and (4.20), yielding

$$\begin{aligned}h_{\epsilon 0}\sim{}&\bar{y}_\epsilon-\overline{Y}_{\epsilon 000}+\frac{\epsilon\bar{x}_\epsilon^2}{2}A_{000}-\epsilon[\bar{y}_\epsilon-\overline{Y}_{\epsilon 000}]\left[\tfrac{1}{2}+\frac{1}{\pi}\tan^{-1}\frac{\bar{x}_\epsilon}{\bar{y}_\epsilon-\overline{Y}_{\epsilon 000}}\right]\\&+\frac{\epsilon w_{0c2}}{2}-\frac{\epsilon\bar{x}_\epsilon}{2\pi}(-2+\ln[\bar{x}_\epsilon^2+(\bar{y}_\epsilon-\overline{Y}_{\epsilon 000})^2])-\frac{L_\epsilon^2 A_{000}\epsilon}{4}\\&+\frac{\epsilon C_0}{2}\ln\frac{4}{L_\epsilon^2}[\bar{x}_\epsilon^2+(\bar{y}_\epsilon-\overline{Y}_{\epsilon 000})^2]+\frac{2C_1\bar{x}_\epsilon\epsilon}{L_\epsilon}+\frac{4\epsilon C_2}{L_\epsilon^2}[-\bar{x}_\epsilon^2+[\bar{y}_\epsilon-\overline{Y}_{\epsilon 000}]^2],\end{aligned}$$

where we have anticipated the fact that $\{C_{2k+1}=0: k=1,2,\ldots\}$, and we have neglected terms that are small as $\bar{x}_\epsilon^2+\bar{y}_\epsilon^2\to\infty$. Changing to the outer variables, and retaining only terms of order less than or equal to ϵ as $\epsilon\to 0$, gives

$$\begin{aligned}h_0\sim{}&\bar{y}+\frac{\bar{x}^2}{2}A_{000}+\frac{4C_2}{L_\epsilon^2}(-\bar{x}^2+\bar{y}^2)+\frac{\bar{x}}{\pi}\epsilon\ln\epsilon+\epsilon\left[-\frac{\bar{y}}{2}-\frac{\bar{y}}{\pi}\tan^{-1}\frac{\bar{x}}{\bar{y}}\right.\\&\left.-\frac{\bar{x}}{2\pi}\{-2+\ln(\bar{x}^2+\bar{y}^2)\}+\frac{2C_1\bar{x}}{L_\epsilon}-\overline{Y}_{\epsilon 000}-\frac{8C_2\overline{Y}_{\epsilon 000}\bar{y}}{L_\epsilon^2}\right]+\ldots.\end{aligned} \tag{4.38}$$

Unfortunately, it is a little awkward to obtain the local form of the *outer solution* in the vicinity of $r=1$, $\phi=\frac{1}{2}\pi$ using the form of the solution derived in §4.2. This is a direct consequence of the fact that the series appearing in (4.10) does not converge uniformly. However, it is a fairly straightforward procedure to derive an analytic solution for h_{0c1} valid *only* in the neighbourhood of $r=1$, $\phi=\frac{1}{2}\pi$.

The local form of the outer solution valid to $O(\epsilon)$ as $\epsilon \to 0$, is

$$h_0 \sim \bar{y} + \tfrac{1}{2}A_{000}\bar{x}^2 - \tfrac{1}{2}(A_{000}+1)(\bar{x}^2-\bar{y}^2) - L_1 I_1(T^{\frac{1}{2}})\bar{x}\epsilon \ln \epsilon + \epsilon\Big[N_1\bar{x} - (A_{000}+1)\bar{y}\,\overline{Y}_{000} - \overline{Y}_{000} - \bar{y}\Big(\tfrac{1}{2} + \frac{1}{\pi}\tan^{-1}\frac{\bar{x}}{\bar{y}}\Big) - \frac{\bar{x}}{2\pi}\ln(\bar{x}^2+\bar{y}^2) + \frac{\bar{x}}{\pi}\Big] + \ldots, \quad (4.39)$$

$$\overline{Y}_{000} = \frac{-A_{0c1}[I_1(T^{\frac{1}{2}})]^2 + T^{\frac{1}{2}}I_1(T^{\frac{1}{2}})\,I_0(T^{\frac{1}{2}})}{TI_0(T^{\frac{1}{2}})\,[I_0(T^{\frac{1}{2}}) + I_2(T^{\frac{1}{2}})] - 2T[I_1(T^{\frac{1}{2}})]^2}, \quad (4.40)$$

$$N_1 = \lim_{\phi \to \frac{1}{2}\pi}\Big[-B_1 I_1(T^{\frac{1}{2}}) - \frac{1}{\pi} - \frac{G_{c1}}{T} + \frac{1}{2\pi}\ln[\cos\phi]^2 - \sum_{n=1}^{\infty} B_{2n+1} I_{2n+1}(T^{\frac{1}{2}})\frac{\cos(2n+1)\phi}{\cos\phi}\Big]. \quad (4.41)$$

Either N_1 or B_1 can be regarded as unknown; at this point, it is more convenient for N_1 to appear in (4.39).

Requiring (4.38) and (4.39) to be the same gives rise to the following:

$$\frac{4C_2}{L_\epsilon^2} = \frac{A_{000}+1}{2}, \quad -L_1 I_1(T^{\frac{1}{2}}) = \frac{1}{\pi}, \quad \frac{2C_1}{L_\epsilon} = N_1,$$

$$\overline{Y}_{\epsilon 000} = \overline{Y}_{000}, \quad \frac{8C_2\,\overline{Y}_{\epsilon 000}}{L_\epsilon^2} = (A_{000}+1)\,\overline{Y}_{000}.$$

Combining the above with (4.35) and (4.36) gives

$$C_0 = \tfrac{1}{2}L_\epsilon^2, \quad C_1 = \frac{L_\epsilon}{2\pi}\ln\frac{L_\epsilon}{2}, \quad C_2 = \tfrac{1}{8}L_\epsilon^2(A_{000}+1),$$

$$L_1 = \frac{-1}{\pi I_1(T^{\frac{1}{2}})}, \quad N_1 = \frac{1}{\pi}\ln\frac{L_\epsilon}{2}.$$

The remaining constant L_ϵ is determined by (4.32) and (4.37). Substituting the above expression for C_0 into (4.37) gives $-L_\epsilon/\pi \geqslant -L_\epsilon^2$. This implies that $L_\epsilon \geqslant 1/\pi$. However, (4.32) demands that $L_\epsilon \leqslant 1/\pi$. Hence the only possibility is that $L_\epsilon = 1/\pi$.

Since the value of N_1 has been explicitly determined, (4.41) may be used to obtain $B_1(T)$. This has been done numerically (refer to figure 7 and Appendix B).

5. The steady motion of a drop moving down an inclined plane with contact-angle hysteresis

It is fairly straightforward to show that the leading terms in an asymptotic expansion, valid in the limit as $\epsilon \to 0$, are given by the various modes identified in §§ 3 and 4. The expansions of the dependent variable and unknown parameters are most easily appreciated by identifying them in two steps. Since we are interested in describing the steady motion of a drop moving down an inclined plane, the value of G must be greater than G_c. Hence we can begin by expanding the various quantities in terms of the small parameter $G - G_c$ as follows:

$$h_0(r,\phi;G,\epsilon,T,\kappa_A/\kappa_R) \sim h_{0c}(r,\phi;\epsilon,T) + (G-G_c)\,h_{01}(r,\phi;\epsilon,T,\kappa_A/\kappa_R) + \ldots, \quad (5.1a)$$

$$A_0(G,\epsilon,T,\kappa_A/\kappa_R) \sim A_{0c}(\epsilon,T) + (G-G_c)\,A_{01}(\epsilon,T,\kappa_A/\kappa_R) + \ldots, \quad (5.1b)$$

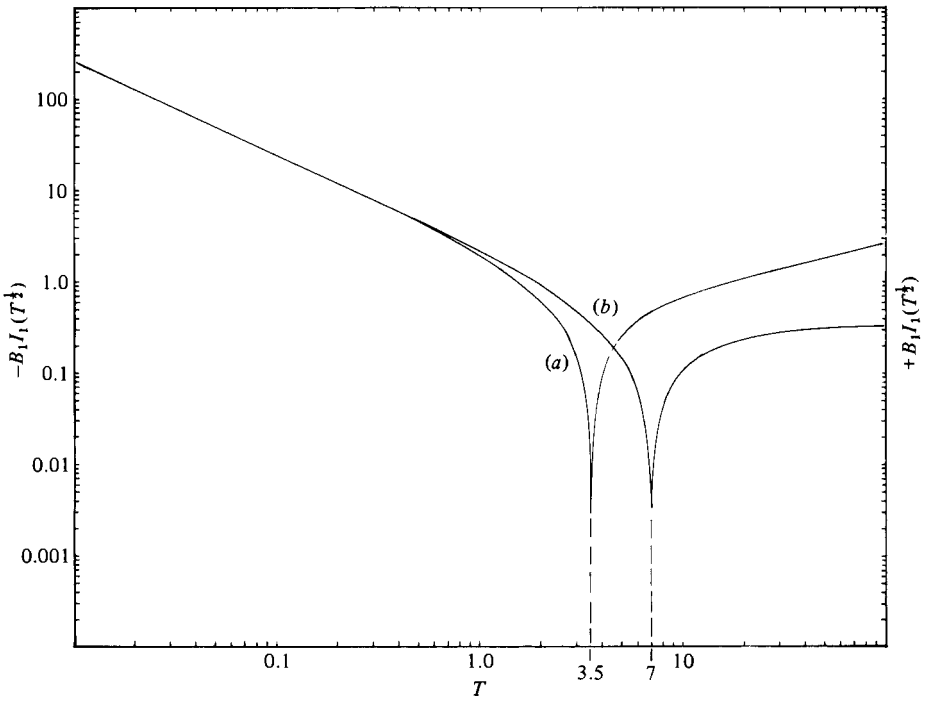

FIGURE 7. Curve (*a*) indicates the value of $B_1 I_1(T^{\frac{1}{4}})$ evaluated numerically. Curve (*b*) is its asymptotic form valid for small values of T given by (B 2).

$$\phi_{A0}(G, \epsilon, T, \kappa_A/\kappa_R) \sim \phi_{A0c}(\epsilon, T) + (G - G_c)\,\phi_{A01}(\epsilon, T, \kappa_A/\kappa_R) + \ldots, \tag{5.1c}$$

$$\phi_{R0}(G, \epsilon, T, \kappa_A/\kappa_R) \sim \phi_{R0c}(\epsilon, T) + (G - G_c)\,\phi_{R01}(\epsilon, T) + \ldots, \tag{5.1d}$$

$$\boldsymbol{U}_{P0}(G, \epsilon, T, \kappa_A/\kappa_R) \sim \mathbf{0} + (G - G_c)\,\boldsymbol{U}_{P01}(\epsilon, T, \kappa_A/\kappa_R) + \ldots, \tag{5.1e}$$

valid in the limit as $G \to G_c$. When $G - G_c = 0$, the drop is in its critical configuration, hence $\{h_{0c}, A_{0c}, \phi_{A0c}, \phi_{R0c}\}$ corresponds to the problem analysed in §4.

The final step consists of identifying the appropriate expansions for $\{h_{0c}, A_{0c}, \phi_{A0c}, \phi_{R0c}\}$, $\{h_{01}, A_{01}, \phi_{A01}, \phi_{R01}, \boldsymbol{U}_{P01}\}$ and G_c in terms of ϵ. The appropriate expansions for the first set of terms, and the parameter G_c, has already been established in §4. If the expansions of the second group of terms are assumed to have the form

$$\begin{aligned}
h_{01}(r, \phi; \epsilon, T, \kappa_A/\kappa_R) &= h_{010}(r, \phi; T, \kappa_A/\kappa_R) + o(1), \\
A_{01}(\epsilon, T, \kappa_A/\kappa_R) &= A_{010}(T, \kappa_A/\kappa_R) + o(1), \\
\phi_{A01}(\epsilon, T, \kappa_A/\kappa_R) &= \phi_{A010}(T, \kappa_A/\kappa_R) + o(1), \\
\phi_{R01}(\epsilon, T, \kappa_A/\kappa_R) &= \phi_{R010}(T, \kappa_A/\kappa_R) + o(1), \\
\boldsymbol{U}_{P01}(\epsilon, T, \kappa_A/\kappa_R) &= \boldsymbol{U}_{P010}(T, \kappa_A/\kappa_R) + o(1),
\end{aligned}$$

valid in the limit as $\epsilon \to 0$, then the lowest-order mode must correspond to the problem analysed in §3. This follows from the fact that the expansions appearing in (5.1*a–e*) are valid when $\epsilon \equiv 0$, which is by definition the problem analysed in §3. Hence both ϕ_{A010} and ϕ_{R010} are equal to zero.

In summary, when $0 < \epsilon \ll 1$ and $0 < G - G_c \ll 1$ the solution has the form

$$h_0 \sim h_{000}(r, \phi; T) + \epsilon \ln \epsilon\, h_{0cL}(r, \phi; T) + \epsilon h_{0c1}(r, \phi; T) + [G - \epsilon G_{c1}(T)]\, h_{010}(r, \phi; T, \kappa_A/\kappa_R) + \ldots,$$

$$A_0 \sim A_{000}(T) + \epsilon A_{0c1}(T) + [G - \epsilon G_{c1}(T)]\, A_{010}(T, \kappa_A/\kappa_R) + \ldots,$$

$$\phi_{A0} \sim \tfrac{1}{2}\pi + \epsilon \phi_{A0c1} + \ldots,$$

$$\phi_{R0} \sim \tfrac{1}{2}\pi + \epsilon \phi_{R0c1} + \ldots,$$

$$U_{P0} \sim [G - \epsilon G_{c1}(T)]\, U_{P010}(T, \kappa_A/\kappa_R) + \ldots,$$

valid in the limit as $\epsilon \to 0$.

6. Results and discussion

The results derived in the preceding sections can be used to solve some of the problems identified in §1, subject, of course, to the limitations imposed by both the small-slope approximation and $\epsilon \ll 1$.

Let us begin by determining the volume of the largest drop that can stick to a solid, assuming that θ_A, θ_R, $\sigma/\rho g$, and γ are all specified. However, before V can be calculated, the value of the scale a must be determined (refer to (2.21)). This can be accomplished by using the relationship obtained upon substituting the value of G_{c1}, given by (4.11), into $G \sim \epsilon G_{c1}$:

$$\tan \gamma = \epsilon \theta_A \frac{2}{\pi} \frac{I_1(T^{\frac{1}{2}})}{T^{\frac{1}{2}} I_2(T^{\frac{1}{2}})}, \tag{6.1}$$

where γ is equivalent to γ_c for this problem. Since γ, θ_A and θ_R are known, (6.1) can be used to calculate T. The value of a follows directly from the definition of T. For convenience, the solution of (6.1) is provided in figure 8 for various values of $\epsilon\theta_A$. The parameter B_d, defined as $\rho g a^2/\sigma$, appearing in the figure, is a convenient dimensionless form for a. It is often referred to as the Bond number. Upon expanding the right-hand side of (6.1) asymptotically for both $T \to 0$ and $T \to \infty$, two approximate forms of the solution are obtained:

$$B_d \sim \epsilon \theta_A \frac{8}{\pi \sin \gamma}, \tag{6.2}$$

$$B_d \sim \frac{1}{\cos \gamma} \left\{ \frac{15}{16} + \frac{\epsilon \theta_A}{\pi \tan \gamma} + \left[\left(\frac{15}{16} + \frac{\epsilon \theta_A}{\pi \tan \gamma} \right)^2 - \frac{3 \epsilon \theta_A}{4 \pi \tan \gamma} \right]^{\frac{1}{2}} \right\}^2, \tag{6.3}$$

valid in the limits $T \to 0$ and $T \to \infty$ respectively. Note that $T \to 0$ corresponds to either $\gamma \to 90°$ or $B_d \to 0$; while $T \to \infty$ corresponds to $B_d \to \infty$. The calculation for V is completed by combining the above results with (2.21). This eliminates the presence of the scale a, and yields an explicit relationship between the dimensionless volume $V/\pi\theta_A(\sigma/\rho g)^{\frac{3}{2}}$ and γ (refer to figure 9). The leading terms of asymptotic expansions of this relationship are

$$\frac{V}{\pi \theta_A (\sigma/\rho g)^{\frac{3}{2}}} \sim 2 \left(\frac{2 \epsilon \theta_A}{\pi \sin \gamma} \right)^{\frac{3}{2}}, \tag{6.4}$$

$$\frac{V}{\pi \theta_A (\sigma/\rho g)^{\frac{3}{2}}} \sim \frac{1}{(\cos \gamma)^{\frac{3}{2}}} [B_d \cos \gamma - \tfrac{3}{2} (B_d \cos \gamma)^{\frac{1}{2}}], \tag{6.5}$$

valid in the limits $T \to 0$ and $T \to \infty$ respectively, where (6.3) must be substituted into (6.5) in order to obtain its final form. It is worth noting that B_d represents, to lowest order, a dimensionless form of the area πa^2 of the solid wetted by the drop, in addition to providing necessary information for determining the volume of the largest drop.

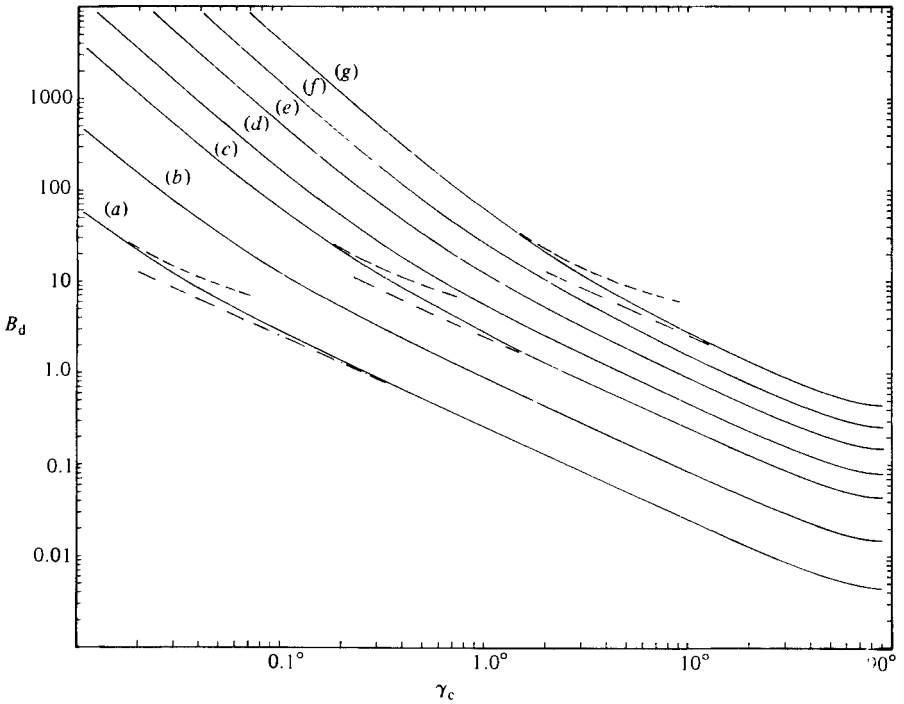

FIGURE 8. Equation (6.1) is evaluated for different values of $\epsilon\theta_A$; $\epsilon\theta_A = 0.1°$ for (*a*), 0.337° for (*b*), 1.0° for (*c*), 1.88° for (*d*), 3.37° for (*e*), 5.84° for (*f*), 10° for *g*. Curves denoted by – – – – – and —·— are obtained by evaluating (6.3) and (6.2) respectively. This is only valid when the drop is in its critical static configuration.

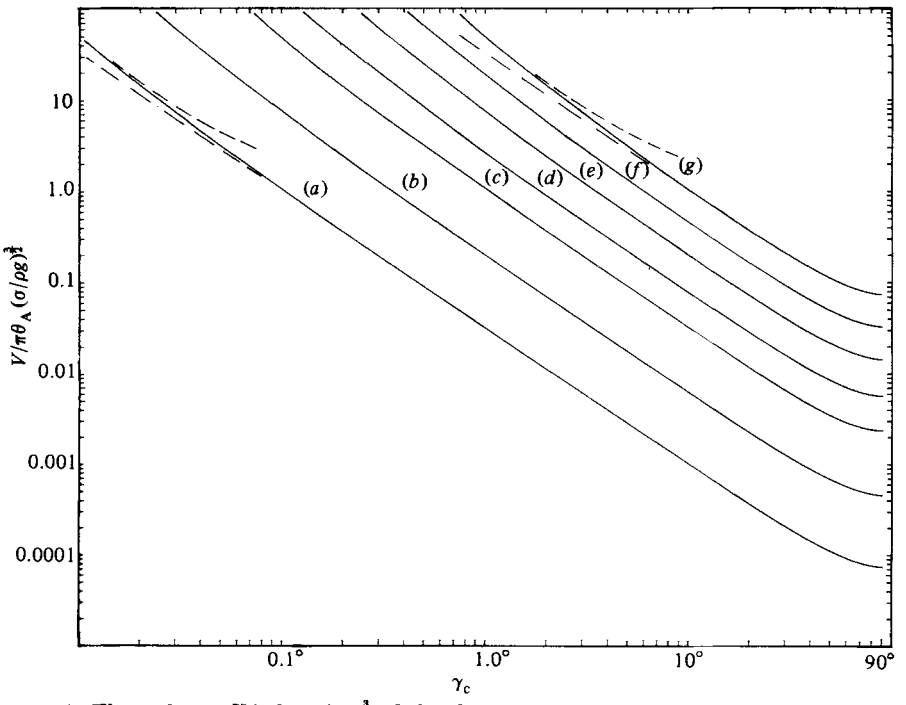

FIGURE 9. The volume $V/\pi\theta_A(\sigma/\rho g)^{\frac{3}{2}}$ of the drop in its critical static configuration is evaluated at different angles of inclination γ_c for the same values of $\epsilon\theta_A$ as in figure 8. The curves denoted by – – – – – and —·— are obtained by evaluating (6.5) and (6.4) respectively.

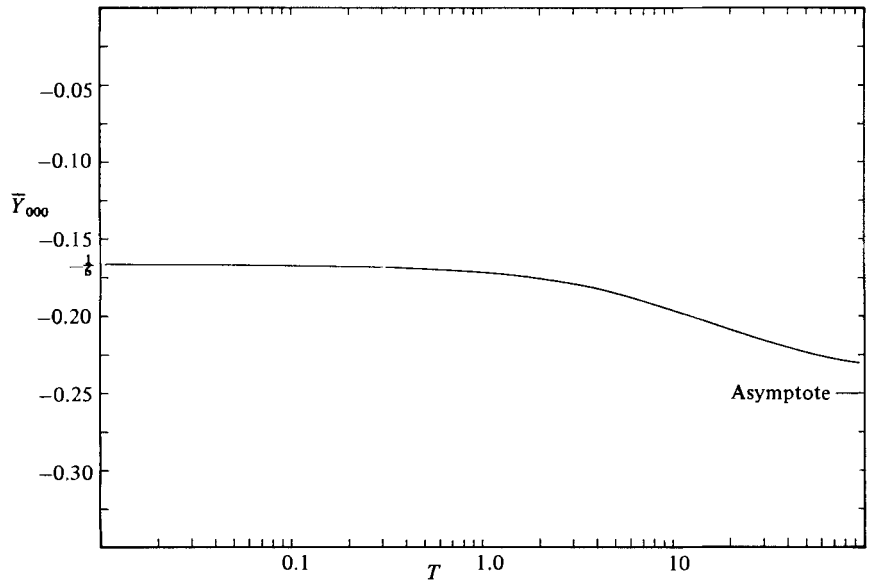

FIGURE 10. The width of the drop in its critical static configuration is obtained directly from (6.6) by using $\bar{Y}_{000}$.

It is also of interest to determine the shape of the drop in its critical configuration. The existence of straight-line segments in the contact line along its sides has already been discussed in §§1 and 2. In order for the solution presented in §4 to be consistent with the small-slope approximation, it was found that the length of these segments must equal $2\epsilon a/\pi$. In spite of the existence of these segments, it is surprising to find, upon evaluating (4.16) at $\phi = 0, \frac{1}{2}\pi, \pi$ and $\frac{3}{2}\pi$, that the length and width of the drop are equal, at least to $O(\epsilon)$ as $\epsilon \to 0$. Their value is given by $2a - 2a\epsilon \bar{Y}_{000}$. Substituting (4.15) into (4.40) yields

$$\bar{Y}_{000} = \frac{1}{T^{\frac{1}{2}}} \frac{I_1(T^{\frac{1}{2}})\, I_2(T^{\frac{1}{2}})}{I_2(T^{\frac{1}{2}})\,[I_0(T^{\frac{1}{2}}) + I_2(T^{\frac{1}{2}})] - 2[I_1(T^{\frac{1}{2}})]^2} \tag{6.6}$$

(refer to figure 10). It can readily be shown that $\bar{Y}_{000} \to -\frac{1}{6}$ as $T \to 0$, and that $\bar{Y}_{000} \to -\frac{1}{4}$ as $T \to \infty$. The asymmetry induced by the contact-angle hysteresis takes the form of unequal distances between the origin (refer to figure 5) and the front and rear of the drop. The degree to which this occurs can be quantified by $R_0(0) - \frac{1}{2}[R_0(0) + R_0(\pi)]$, which will be referred to as δ_0. It value, to $O(\epsilon)$ as $\epsilon \to 0$, can be evaluated directly by using (4.16), giving

$$\delta_{0c} \sim \frac{a\epsilon}{\pi}\left[\ln\frac{2\pi}{\epsilon} + \frac{\pi}{2} - 2\right] \tag{6.7}$$

as $T \to 0$. Thus, for small values of ϵ, δ is positive, indicating that the drop 'droops forward' in its critical configuration.

When V and γ take on values resulting in $G > G_c$, the drop must be moving down the surface. Before calculating either G or G_{c1}, it is necessary to evaluate the scale a. Since the values of both V and γ are known, the value of a can be calculated directly from (2.21). For convenience, this equation is presented in figure 11, which illustrates the dependence of $V/\pi\theta_A(\sigma/\rho g \cos\gamma)^{\frac{1}{2}}$ on the variable T. Knowledge of the value of T determines G by the expression $(T \tan\gamma)/\theta_A$, and determines G_{c1} by (4.11) or figure 12. Having calculated both G and G_{c1}, the speed at which the drop moves down the surface when it achieves steady state, U_{D0}, in dimensional form, can easily be

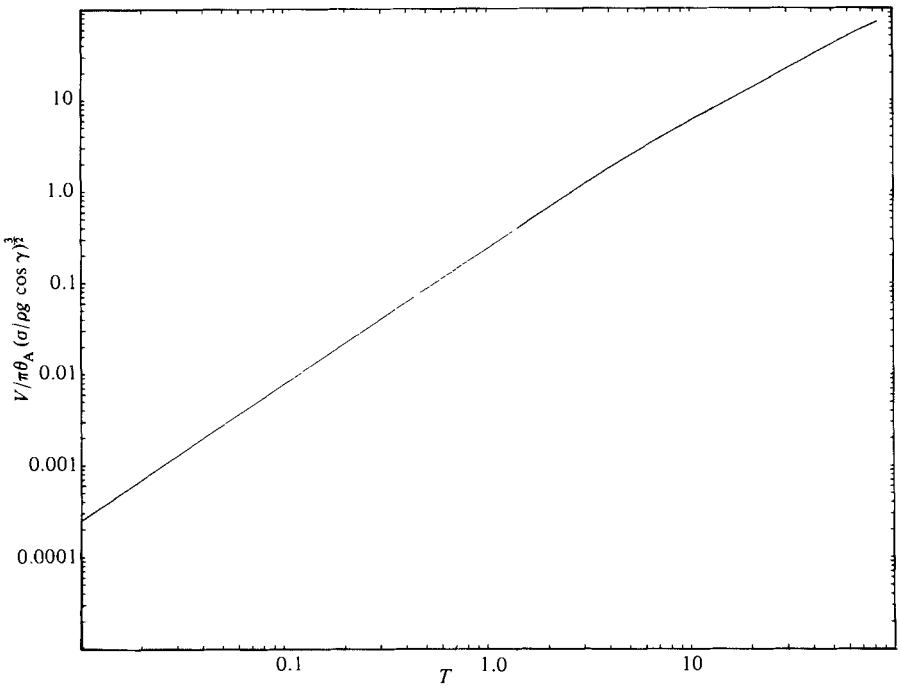

FIGURE 11. The dependence of $V/\pi\theta_A(\sigma/\rho g\cos\gamma)^{\frac{3}{2}}$ on T calculated directly from (2.21). The relationship is valid whether or not the drop is in its critical configuration.

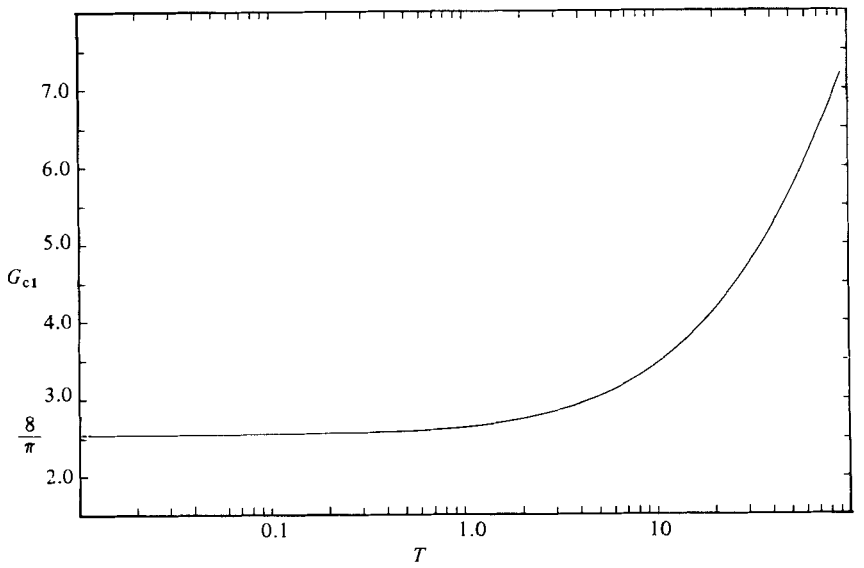

FIGURE 12. The variation of G_{c1} with T.

evaluated from $-U_{P010}\kappa_A\theta_A(G-\epsilon G_{c1})$. Upon substituting (3.11) into this expression, it is found, to lowest order, that

$$U_{D0} \sim \frac{2V}{\pi a^3(1/\kappa_A+1/\kappa_A)}(G-\epsilon G_{01}). \tag{6.8}$$

Note that a large positive value of $d\theta/dU$ for *either* $U > 0$ or $U < 0$ (equivalent for $1/\kappa_A$ or $1/\kappa_R$), results in a slowly moving drop. Negative values of $d\theta/dU$ can cause

a drop to move *up* the surface of the solid, a violation, one might suspect, of the second law of thermodynamics!† For material systems in which the values of $\mathrm{d}\theta/\mathrm{d}U$ are near zero for *both* $U \gtrless 0$, thus resulting in a large value of $\mu U_0/\sigma$, (6.8) is no longer valid because the viscous forces created by the motion of the liquid within the drop are no longer negligible.

The manner in which the dynamics of the drop affects its shape is also somewhat interesting. To lowest order, its length L_{D} and width ω are no longer equal. It can easily be shown that, in the limit as $T \to 0$,

$$L_{\mathrm{D}} \sim 2a - 2a\epsilon\,\overline{Y}_{000} - \frac{a}{\pi}\left(G - \frac{\epsilon 8}{\pi}\right)\left(\bar{G} + \frac{5}{6} - \frac{\pi}{4}\right)\frac{\kappa_{\mathrm{R}} - \kappa_{\mathrm{A}}}{\kappa_{\mathrm{R}} + \kappa_{\mathrm{A}}}, \tag{6.9}$$

$$\omega \sim 2a - 2a\epsilon\,\overline{Y}_{000} + \frac{a}{\pi}\left(G - \frac{\epsilon 8}{\pi}\right)\left(\frac{\pi^2}{8} - \frac{5}{6}\right)\frac{\kappa_{\mathrm{R}} - \kappa_{\mathrm{A}}}{\kappa_{\mathrm{R}} + \kappa_{\mathrm{A}}},$$

where $\bar{G}$, Catalan's constant, equals 0.915965594177219015... (Abramowitz & Stegun 1964). Since both constants $\bar{G} + \frac{5}{6} - \frac{1}{4}\pi$ and $\frac{1}{8}\pi^2 - \frac{5}{6}$ are positive, the relative sizes of L_{D} and ω depend on the relative values of κ_{A} and κ_{R}; if $1/\kappa_{\mathrm{A}} > 1/\kappa_{\mathrm{R}}$, i.e. $\mathrm{d}\theta/\mathrm{d}U$ for $U > 0$ is larger than $\mathrm{d}\theta/\mathrm{d}U$ for $U < 0$, than the drop is wider than it is long, $\omega > L_{\mathrm{D}}$; while $1/\kappa_{\mathrm{R}} > 1/\kappa_{\mathrm{A}}$ creates a drop that is longer than it is wide, $L_{\mathrm{D}} > \omega$. On the other hand, the value of δ_0 is unaffected by the motion of the drop, retaining the same value given by (6.7).

Finally, as suggested in §1, it is not difficult to construct schemes for deducing the values of θ_{A}, θ_{R}, κ_{A} and κ_{R} based upon measuring various characteristics of the drop. For example, by placing a drop of known volume on a surface, and measuring its length and angle of inclination when it is in its critical configuration, (2.21), (6.1) and (6.6) can be used to determine θ_{A} and θ_{R}. Once θ_{A} and θ_{R} are known, (6.8), (6.9), and either (2.21) or figure 11 can be used to calculate κ_{A} and κ_{R} from measurements of U_{D} and L_{D} for a drop of known volume placed on a surface inclined at a specified angle.

We would like to acknowledge Bruce Lawrey and Ben Dussan V. for their efforts in the preparation of the various graphs and to extend a special thanks to Wei-Kuang Chi for his numerical work in the evaluation of B_1.

This work was supported in part by the U.S. Army Research office under grant DAAG 29-82-K-0128.

Appendix A. Force balance on a drop in its critical static configuration

Let us sum the forces acting on the material body $\mathscr{V}$ indicated in figure 13 by the dashed line. We need only be concerned with the two components tangent to the plane of the surface of the solid. It follows directly that

$$0 = \int_{\mathscr{C}} \sigma(\boldsymbol{M}\cdot\mathbf{m})\,\boldsymbol{m}\,\mathrm{d}l + \rho g\, V \sin\gamma_{\mathrm{c}}\,\boldsymbol{i}, \tag{A 1}$$

where $\mathscr{C}$ denotes the location of the contact line, a differential length of which is given by $\mathrm{d}l$, and $\boldsymbol{M}$ and $\boldsymbol{m}$ are unit vectors whose directions are indicated in figures 13 and 4 respectively.

We next make use of the definition of the contact angle,

$$\cos\theta \equiv \boldsymbol{M}\cdot\boldsymbol{m}.$$

† The authors are unaware of any experimental measurements in which $\mathrm{d}\theta/\mathrm{d}U$ takes on negative values for either the advancing or receding contact line.

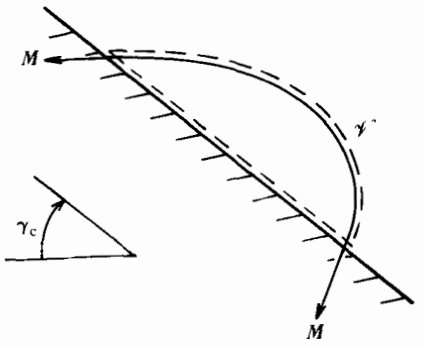

FIGURE 13. A side view of the drop in its critical static configuration. The boundary of γ is located within the gas, just beyond the interface, and within the drop, a bit above the solid. The unit vector $\boldsymbol{M}$ is embedded in the local tangent plane of the gas–liquid interface, perpendicular to the vector tangent to the contact line, and pointing away from the drop.

The integration along the contact line can be divided into four segments: the advancing $\mathscr{C}_A$ and receding $\mathscr{C}_R$ portions, along which the contact angle take on the constant values of θ_A and θ_R respectively; and the two straight lines on the sides of the drop (see figure 4). Owing to symmetry the $\boldsymbol{j}$-component of integration must be zero; hence (A 1) can be rewritten as

$$0 = \sigma\cos\theta_A\int_{\mathscr{C}_A}\boldsymbol{m}\cdot\boldsymbol{i}\,dl+\sigma\cos\theta_R\int_{\mathscr{C}_R}\boldsymbol{m}\cdot\boldsymbol{i}\,dl+\rho g V\sin\gamma.$$

The derivation of (1.1) is completed upon making the identification

$$\omega = \int_{\mathscr{C}_A}\boldsymbol{m}\cdot\boldsymbol{i}\,dl = -\int_{\mathscr{C}_R}\boldsymbol{m}\cdot\boldsymbol{i}\,dl.$$

Furmidge (1962) simplifies his derivation by assuming that the contact line is rectangular in shape. Thus he refers to (1.1) as an approximation that to his surprise agrees remarkably well with his experimental measurements!

Appendix B. Determination of $B_1(T)$

The value of $B_1(T)$ is obtained from the following limit:

$$B_1 I_1(T^{\frac{1}{2}}) = \lim_{\phi\to\frac{1}{2}\pi}\left\{\frac{1}{2\pi}\ln(\cos\phi)^2-\sum_{n=1}^{\infty}B_{2n+1}I_{2n+1}(T^{\frac{1}{2}})\frac{\cos(2n+1)\phi}{\cos\phi}\right\}-\frac{G_{c1}}{T}+\frac{1}{\pi}\ln 2\pi-\frac{1}{\pi},$$

where G_{c1} and $\{B_{2n+1}: n = 1, 2, \ldots\}$ are given by (4.11) and (4.13) respectively. With a little effort, it can be shown that

$$\sum_{n=1}^{\infty}\frac{(-1)^{n+1}}{2\pi n^2}\frac{\cos(2n+1)\phi}{\cos\phi}\sim\frac{1}{2\pi}\ln(\cos\phi)^2+\frac{1}{\pi}(\ln 2-1)-\frac{\pi}{2}\quad\text{as}\quad\phi\to\tfrac{1}{2}\pi.$$

Substituting this into the above expression gives

$$B_1 I_1(T^{\frac{1}{2}})+\frac{G_{c1}}{T}-\frac{1}{\pi}\ln\pi-\frac{\pi}{2}=\lim_{\phi\to\frac{1}{2}\pi}\sum_{n=1}^{\infty}\left[\frac{(-1)^{n+1}}{2\pi n^2}-B_{2n+1}I_{2n+1}(T^{\frac{1}{2}})\right]\frac{\cos(2n+1)\phi}{\cos\phi}.$$

The singularity has thus been removed from the summation. Since the convergence is now uniform, l'Hôpital's rule can be used to give

$$B_1 I_1(T^{\frac{1}{2}})+\frac{G_{c1}}{T}-\frac{\ln\pi}{\pi}-\frac{\pi}{2}=\sum_{n=1}^{\infty}\left[\frac{(-1)^{n+1}}{2\pi n^2}-B_{2n+1}I_{2n+1}(T^{\frac{1}{2}})\right](2n+1)(-1)^n. \quad \text{(B 1)}$$

In the limit as $T \to 0$ it is easily shown that

$$B_1 I_1(T^{\frac{1}{2}}) \sim \frac{1}{\pi} \ln \pi - \frac{8}{\pi T}. \tag{B 2}$$

In general, the convergence of the series in (B 1) is fairly rapid and can readily be evaluated numerically over a relatively wide range of T (see figure 7). Note that it agrees well with the asymptotic expression given by (B 2) for $T \lesssim 0.3$.

REFERENCES

ABRAMOWITZ, M. & STEGUN, I. A. 1964 *Handbook of Mathematical Functions.* NBS Applied Maths Series 55.

BIKERMAN, J. J. 1950 Sliding of drops from surfaces of different roughnesses. *J. Colloid Sci.* **5**, 349.

BLAKE, T. D. & HAYNES, J. M. 1969 Kinetics of liquid/liquid displacement. *J. Colloid Interface Sci.* **30**, 421.

BROWN, R. A., ORR, F. M. & SCRIVEN, L. E. 1980 Static drop on an inclined plate: analysis by the finite element method. *J. Colloid Interface Sci.* **73**, 76.

DUSSAN V., E. B. 1976 The moving contact line: the slip boundary condition. *J. Fluid Mech.* **77**, 665.

FURMIDGE, C. G. L. 1962 Studies at phase interfaces. I. The sliding of liquid drops on solid surfaces and a theory for spray retention. *J. Colloid Sci.* **17**, 309.

GREENSPAN, H. P. 1978 On the motion of a small viscous droplet that wets a surface. *J. Fluid Mech.* **84**, 125.

HANSEN, R. J. & TOONG, T. Y. 1971 Dynamic contact angle and its relationship to forces of hydrodynamic origin. *J. Colloid Interface Sci.* **37**, 196.

HOCKING, L. M. 1981 Sliding and spreading of thin two-dimensional drops. *Q. J. Mech. Appl. Maths* **34**, 37.

HUH, C. & MASON, S. G. 1977 The steady movement of a liquid meniscus in a capillary tube. *J. Fluid Mech.* **81**, 401.

JOHNSON, D. R. 1973 Spreading and retention of agricultural sprays on foliage. *Pesticide Formulations* (ed. W. VanValkenburg), p. 343. Marcel Dekker.

KAFKA, F. Y. & DUSSAN V., E. B. 1979 On the interpretation of the dynamic contact angle in capillaries. *J. Fluid Mech.* **95**, 539.

LOWNDES, J. 1980 The numerical simulation of the steady movement of a fluid meniscus in a capillary tube. *J. Fluid Mech.* **101**, 631.

MACDOUGALL, G. & OCKRENT, C. 1942 The adhesion of liquids to solids and a new method of determining the surface tension of liquids. *Proc. R. Soc. Lond.* A **180**, 151.

NEUMANN, A. W., ABDELMESSIH, A. J. & HAMEED, A. 1978 The role of contact angles and contact angle hysteresis in dropwise condensation heat transfer. *Intl J. Heat Mass Transfer* **21**, 947.

NGAN, C. G. & DUSSAN V., E. B. 1982 On the nature of the dynamic contact angle: an experimental study. *J. Fluid Mech.* **118**, 27.

SADHAL, S. S. & PLESSET, M. S. 1979 Effect of solid properties and contact angle in dropwise condensation and evaporation. *Trans. ASME* C: *J. Heat Transfer* **101**, 48.